Review article

Tutorial review of reverse osmosis and electrodialysis

P.M. Biesheuvel [a], S. Porada [a], M. Elimelech [b], J.E. Dykstra [c,*]

[a] *Wetsus, European Centre of Excellence for Sustainable Water Technology, The Netherlands*
[b] *Department of Chemical and Environmental Engineering, Yale University, USA*
[c] *Environmental Technology, Wageningen University, The Netherlands*

ARTICLE INFO

ABSTRACT

Reverse osmosis (RO) and electrodialysis (ED) are the two most important membrane technologies for water desalination and treatment. Their desalination and transport mechanisms are very different, but on a closer look also have many similarities. In this tutorial review, we describe state-of-the-art theory for both processes, focusing on simple examples that are helpful for the non-specialist and for classroom teaching. We describe relevant theory for ion and water transport and the coupling with theory for chemical and mechanical equilibrium on membrane/solution interfaces. For RO of neutral solutes, we explain the solution-friction (SF) model which is closely related to the classical sieving or pore flow model. The SF model includes advection, diffusion, and solute partitioning, and leads to simple relationships for the coupled fluxes of water and solutes (and thus for solute retention as well), also when a diffusion boundary (or concentration polarization) layer is included in the model. Subsequently this theory is extended to describe RO for symmetric salt solutions with charged membranes. For the desalination of salt solutions, both for RO and ED we present two-dimensional module-scale calculations which lead to a characteristic curve that determines optimum operational conditions based on a simple cost calculation that offsets energy and material costs. We discuss the two-fluid model (TFM) that comprehensively describes ion and water flow both in RO and ED, and we explain how this theory also accurately describes osmosis experiments where water and ions are transported in opposite directions through a membrane. Finally, we present results of optimization studies of the combination of multiple modules for RO and ED, and we evaluate the relevance of concentration polarization by using a 3D model for cross-current flow in an ED module.

1. Introduction

Reverse osmosis (RO) and electrodialysis (ED) are the two most applied membrane methodologies for water treatment and desalination (deionization) [1,2]. A brief schematic of both methods is presented in Fig. 1. Water treatment generally refers to the removal of contaminants other than salts, such as organic micropollutants (OMPs), whereas desalination and deionization refer to the removal of salts, thus of ions. RO is a method that uses pressure to drive water through a membrane, retaining on the retentate side most of the ions and other solutes, producing freshwater on the permeate side.[1] Nanofiltration (NF) is a companion technology of RO that uses lower pressures, and membranes with larger pore sizes than in RO [3,4]. In NF, the retention of monovalent ions is much lower than of divalent ions and thus divalent ions can be selectively removed. In ED, water flows through thin channels next to ion-exchange membranes (IEMs) and an applied current pulls the ions from one set of channels through the IEMs to other channels. The theories that we present for RO and ED, and the relevant metrics that we define, also apply to NF and EDI and other related desalination methods.

Though ED and RO are very different methods and use distinctly different physical mechanisms, our aim is to demonstrate that the underlying transport theory for flow of water and solutes is the same. As we will show, the effects of charge and current that are of key importance in ED, also play a role in RO. Similarly, in ED pressures develop which influence ion and water transport. Thus it is relevant to present a generalized treatment that applies to both process types. We also demonstrate that key performance indicators on the module level, of relevance for (economic) process optimization, are defined for RO and ED in very similar terms, and relate to one another in a similar fashion. The theories that we present for RO and ED, and the relevant metrics that we define, also apply to other desalination methods such as NF and electrodeionization (EDI).

---

* Corresponding author.
 E-mail address: jouke.dykstra@wur.nl (J.E. Dykstra).
 [1] In this work we alternatingly use the words 'ion' and 'solute' for the charged and uncharged species dissolved in the water.
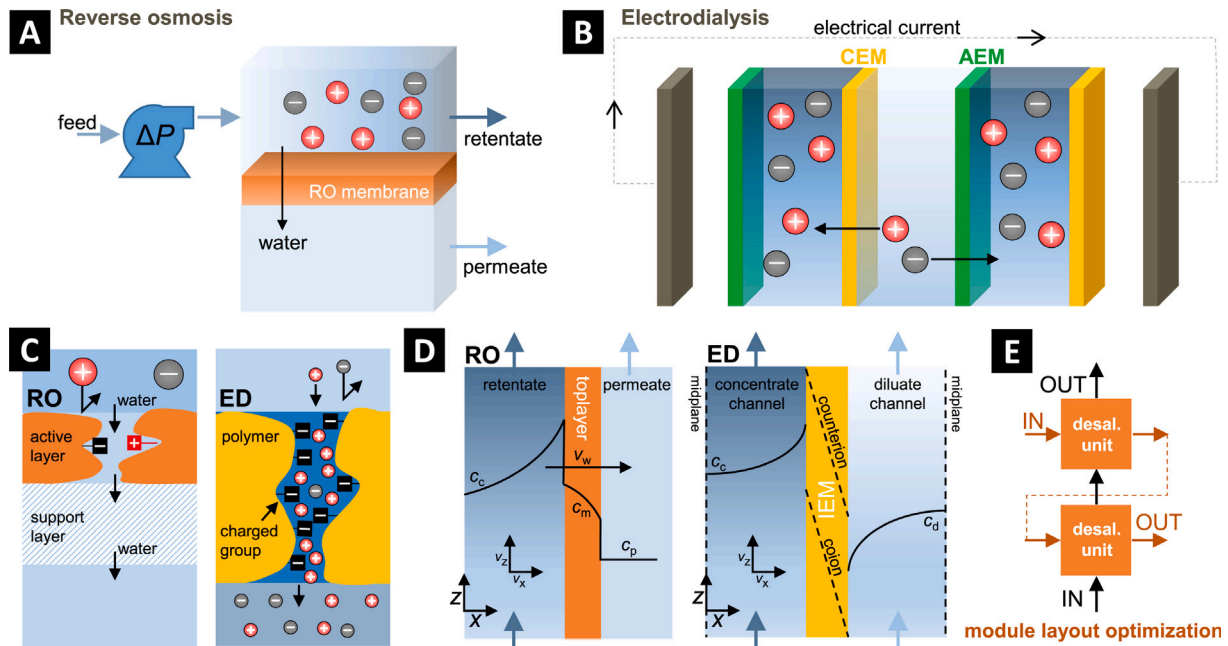
Fig. 1. Overview of reverse osmosis (RO) and electrodialysis (ED). (A) In RO, pressure is applied to drive water through a membrane, retaining on the retentate side most of the solutes. (B) In ED, electrical current runs across channels and membranes, generated in electrodes placed at both ends of a stack that holds many cell pairs. (C) RO and ED have continuous pathways where water and ions move through. The membrane charge and chemical affinity lead to partitioning of solutes on the two outsides of a membrane. (D) On the upstream side of an RO membrane (retentate side), ion concentrations increase towards the membrane (concentration polarization) through a diffusion boundary layer. On the downstream side, freshwater (permeate) is produced. Concentration profiles develop in an ED cell pair with diluate and concentrate channels separated by ion-exchange membranes. (E) Desalination systems can consist of multiple modules of different size, which can be connected in various ways.

In this review we focus on the theory of desalination of ionic solutions, i.e., how to use membranes to obtain freshwater from brackish water or seawater by RO and ED. In Section 2 we describe thermodynamic equations and metrics that apply to both methods. We continue in Section 3 with a discussion of simple models for RO that assume neutral solutes, and we compare the often used solution–diffusion (SD) model with the more accurate solution-friction (SF) model. For the SF model we present analytical solutions for retention, also including the effect of concentration polarization (CP). We also analyze energy efficiency in a 2D flow calculation for an RO module. For ED we discuss in Section 4 a co-current plug flow model valid when several system properties are symmetric. Both for RO and ED we set up in these sections a method of cost calculation that demonstrates why the counter-intuitive result that 'inexpensive membranes have higher energy efficiency' holds true. In Section 5 we describe the general two-fluid model (TFM) and we apply the resulting equations to a novel data set for the osmosis experiment where we have counter-directional salt and water flow, and we explain the origin of the phenomenon of osmosis: *why* does water flow to a solution of high salinity? In Section 6, the theory for RO and ED that we set up earlier, is extended to describe several highly relevant cases. For RO we discuss in this section theory describing retention of ions with charged membranes, and for ED we discuss the effect of flow geometry within an ED system, and the effect of stacking of multiple units. For ED, we also present results of a 3D cross-current calculation including concentration polarization.

We illustrate in Fig. 2 that RO and ED have many aspects in common with one another, which they also have in common with the phenomenon of osmosis. In all these processes, the same three features play a key role, as we discuss next. First, in all cases there are differences in concentration between the two sides of the membrane. Furthermore, there is a certain electrical current, and finally there is a pressure difference across the membrane. In certain cases, the electrical current will be zero, as in RO, and likewise the hydrostatic pressure difference will be (close to) zero in some cases, for instance in the osmosis experiment when the two sides are open to atmosphere and the

		Δc ?	current	ΔP^h ?
Technology	RO/NF	✓	= 0	✓
	ED(I)	✓	✓	~ 0
Phenomenon/experiment	Osmosis	✓	= 0	~ 0

Fig. 2. In reverse osmosis (RO) nanofiltration (NF), electrodialysis (ED), and electrodeionization (EDI), and in the osmosis experiment, salt concentrations on the two sides of the membrane are different, there is an electrical current, and there is a pressure difference. Even when the current or pressure difference is zero or near zero, that information is still an input in the transport models. Thus, on a theoretical level, these three processes are very similar, and a general theory can be used that describes all three processes.

liquid levels about equal. Nevertheless, in the transport theory, current and pressure being zero is a key part of the model structure, i.e., when building a theoretical model, it does not matter very much whether current is zero or non-zero, and in all cases a relation for current is part of the model structure. And the same holds for the pressure difference, unless we do not care about pressure, and assume we know the value of the water velocity (zero or otherwise). Because of these similarities in the required theoretical description for RO, for ED and for osmosis, a combined discussion of these processes is important and insightful.

In this review we necessarily can only address a limited number of topics, and must refer the reader to other literature for many other topics of relevance in RO and ED, such as: ion selectivity in multi-ionic mixtures [5], removal of organic micropollutants [6,7], module and stack design [2], fouling abatement [8], studies of membrane lifetime and robustness, membrane cleaning [9], the design of spacers and membrane geometries [10], and full system-level cost optimization.

2. Thermodynamics and metrics

For all water desalination methods, in all cases the same thermodynamic equations apply, and the same setpoints and metrics (performance indicators) can be used. It is useful to start the discussion with the topic of setpoints and metrics.

2.1. Setpoints and metrics for water desalination

Every water desalination process is defined by certain operational characteristics, i.e., objectives, or setpoints. These are the amount of water to be treated, the water recovery, and the extent of desalination (or salt removal). Different setpoints can be defined but in the end they describe how much freshwater is obtained from how much feedwater, and what is the salt concentration of the product water. These are considered as setpoints and are 'hard' objectives that must be attained.

After the setpoints of a process have been defined, metrics (or, equivalently, 'performance indicators') come into play. They describe optimized operation. Such metrics can be manifold. We can for instance have a measure of energy use (energy efficiency), the degree of removal of specific compounds (selectivity), or a measure of how well the membrane is retaining its integrity over time and able to handle fouling.

2.1.1. Setpoints for water desalination

Setpoints for a water desalination process are operational parameters that are 'hard', that must be attained. It is not the case that they are just 'nice to have', i.e., to be optimized in some direction. Instead, they *define* a certain desalination operation. They are also essential for a calculation of the theoretical minimum energy use (see Section 2.2). In practice, the aim is not that these setpoints are reached in an individual desalination unit (module, stack), but they will be the result of operation of a total desalination plant. So a first module desalinates to a certain percentage, and only in a second module the final salt concentration is reached. In that case, setpoints are only reached at the overall level of a full water desalination plant.

The first setpoint that defines operation of a desalination plant or module, is how much freshwater (diluate, permeate) is obtained in m^3/s, i.e., the freshwater flowrate, $\phi_{v,p}$ (where 'p' refers to permeate or product water). In case operation is not at all times at the same level, one must precisely define whether this capacity refers to an average flowrate, or refers to a peak capacity. In this review we neglect this issue and focus on steady-state operation of one or two modules, with constant flow rates and setpoints.

The second setpoint is water recovery, WR, which is the fraction of all feedwater that is turned into freshwater, thus

$$\text{WR} = \frac{\phi_{v,p}}{\phi_{v,p} + \phi_{v,c}} = \frac{\phi_{v,p}}{\phi_{v,f}} \tag{1}$$

where $\phi_{v,j}$'s are volumetric flowrates in m^3/s. Other terminology is recovery ratio, often described by the symbol r, RR, or α. All flowrates $\phi_{v,j}$ can be replaced here by 'integrated' volumes, V_j. Subscripts 'f', 'p' and 'c' refer to the feedwater, product water (freshwater, or in RO: permeate), and concentrate (retentate), respectively. A related definition is 'split ratio' for the ratio $\phi_{v,p}/\phi_{v,c}$, which equals WR/(1−WR).

The third setpoint is the extent of desalination, which one can define as the difference in salt concentration between feedwater and product water, $\Delta c = c_f - c_p$. Alternatively, the setpoint can simply be the salt concentration of the freshwater that is obtained. Another way to express this setpoint is as a retention, rejection, or passage. Salt retention, R_i, is defined as

$$R_i = 1 - c_{p,i}/c_{f,i}. \tag{2}$$

Retention and rejection have the same meaning, while passage, P_i, is given by $P_i = 1 - R_i$. These latter definitions of R_i and P_i are particularly useful for RO, not so much for ED. The above three setpoints can be

rewritten to other setpoints, but the above formulations are common choices.

In general, we can attain the second and third setpoints in any well-designed RO or ED module, but must then adjust the flowrates of the water treated. Besides the flowrates, in ED we can tune the current density (or voltage) that is applied to a stack. So in most cases, it will be possible to find an operational setting where the second and third setpoints are attained, for a given flow of water that is treated. The same is valid in RO, where we have two flow rates and a pressure difference that can be tuned.

The third setpoint, the degree of desalination, relates to a total or average desalination of the feedwater as a whole. In reality, most water sources contain many different salts, and we aim for a certain separation level of several critical salts amongst all salts. In practice, still, it is useful to treat the desalination as a setpoint, for instance as a 'total Δc' formulated as a summation over all ions, including perhaps a weighing to account that some ions are more relevant to remove than others. The degree of desalination for individual ions, related to ion selectivity, is not a setpoint but a metric.

Thus, for a given module, we can arrive at setpoints for WR and Δc, but this can only be achieved for one (maximum in the) flowrate of the water that is treated. We cannot just achieve any level of the volumetric rate of freshwater that one may desire in a given module, if there are two or more other setpoints to achieve. This can also be rephrased into the statement that the setpoints for WR and Δc determine the ratio of system size (e.g., membrane area) over volume flowrate of the water to be treated (or, to be obtained as freshwater). Let us call this factor the specific membrane area $\mathcal{A}$, i.e., the total membrane area per m^3/s of freshwater to be obtained. Typically, with more stringent setpoints for WR and Δc (i.e, higher WR and Δc), this factor $\mathcal{A}$ will increase, thus more membranes are needed. In addition, also more energy will be required to attain higher WR and Δc. We will quantitatively analyze these predictions in upcoming sections on RO and ED.

2.1.2. Metrics for water desalination

Metrics, or performance indicators, are those factors that for a certain desalination process, defined by certain setpoints, are 'nice to have', that have a value that ideally is as high, or as low, as possible.

A first metric tracks the specific removal of certain key compounds, and the more the removal of these, the better. So a metric could be a removal degree of one or several key ions, perhaps expressed as single number by summing over several key ions including a weighing factor describing the importance of the removal of each.

Another example of a metric is the energy efficiency, η, which is the ratio of the theoretical minimum energy to achieve a certain desalination (defined by the setpoints) over the actual energy investment. (This metric is also called TEE, for 'thermodynamic energy efficiency'.) There are many possible definitions for η, depending on which energy contributions are included in the actual energy input. For instance, for ED we can limit analysis to the electrical energy input required for current to flow across the stack, but we can also include the (much smaller) costs of pumping the water through the channels. In RO we can decide to include for a certain percentage the recovery of 'pressure energy.' We can take into account efficiencies of power sources and pumps, and of other electric equipment, for instance to convert (AC) electricity into pumping power for RO, or into DC stack current for ED [11]. So, a report detailing values of η must carefully lay out which energy factors are considered.

Often, instead of an efficiency η, the inverse factor is reported, which then is the factor by which the actual desalination energy is 'above the minimum'. Generally, values as low as two, for this inverse factor, are considered to be very low, i.e., we now have an actual energy use that is only a factor two above the thermodynamic minimum. In many cases, especially for water of low salinity, this factor is much higher, for instance 5 or 10, which implies the actual energy is equal to that number of times the thermodynamic minimum.

Other metrics may refer to lifetime of the membranes and track the state of membrane functionality and integrity over time. Another metric is total cost of operation. It is clear that many metrics can be defined and used. But important is that setpoints and metrics are clearly defined, both when comparing different materials and operational modes within a certain technology, and when making comparisons between different desalination methods.

2.2. Minimum energy of desalination

For given setpoints, we can calculate the theoretical minimum energy that must be invested to attain that particular degree of desalination. This minimum energy does not depend on what method is used to desalinate. Of course, both in RO and ED there are additional constraints that increase the minimum energy further: for instance, in an RO module we can only apply one pressure, which – on that side of the membrane – is then effective through the entire module. And in an ED stack, there is one value of the cell pair voltage, which then applies in the entire stack. All kinds of modifications are possible to relax these system limitations, especially by working with multiple modules that operate at different conditions. But still, the thermodynamic minimum that we analyze in this section, that is system-independent. This minimum only depends on the composition of the water to be treated, temperature, and setpoints.

This minimum energy that must always be invested to desalinate water, $e_{\min}$, can be calculated on the basis of a thermodynamic analysis of the energy in the three streams that are involved. These three streams are the feedwater 'f', the obtained freshwater (permeate, 'p', or diluate, 'd'), and the concentrate (or, retentate, 'c'). In each stream there are multiple ions, each at a concentration c_i, and all ions are used in the general equations we will discuss first. For a 1:1 salt of one cation and one anion, we can define a salt concentration, c_∞, which is equal to c_i of each of the two ions involved.

2.2.1. The thermodynamics of ideal solutions

For thermodynamically ideal solutions, the only contribution to the theoretical minimum energy of desalination, $e_{\min}$, is the decrease in ion entropy (Gibbs free energy of mixing), and thus $e_{\min} = -T \Delta S$ where

$$\Delta S = S_p + S_c - S_f \tag{3}$$

with the entropy of each stream given by

$$S_j = -R \phi_{v,j} \sum_i c_{i,j} \ln c_{i,j} \tag{4}$$

where R is the gas constant (8.3144 J/mol/K), $\phi_{v,j}$ the volumetric flowrate of a certain stream j (in m^3/s), and $c_{i,j}$ the concentration of ion i in stream j, with $c_{i,j}$ having the unit mol/m^3, i.e., mM.

This equation can be used for any mixture of ions, and irrespective of how successfully each ion is separated in a membrane process. The complete calculation also includes two balances, first a volumetric balance, which is

$$\phi_{v,f} = \phi_{v,p} + \phi_{v,c} \tag{5}$$

and secondly a mass balance per solute type,

$$\phi_{v,f} c_{f,i} = \phi_{v,p} c_{p,i} + \phi_{v,c} c_{c,i} . \tag{6}$$

In setting up the volume balance we assume that the mass density of each of the three streams is the same. A calculation based on these equations is easily performed in spreadsheet software, and results in the input energy in W = J/s required to attain a certain separation in a steady-state process. It can be helpful to interpret $\phi_{v,j}$ as volumes V_j, such that the equation provides the energy in J to treat a certain volume of water. We can define the minimum energy per m^3 of freshwater produced, $E_{\min}$, as $E_{\min} = e_{\min}/\phi_{v,p}$. An important result (to check one's calculation) is that $E_{\min} = 1.0$ kWh per m^3 freshwater produced for a 1:1 salt, with 50% water recovery, i.e., WR = 0.50, a feed salt

concentration $c_\infty = 525$ mM, $c_{\infty,p} = 0$ mM, and temperature $T = 298$ K. Note that a 1:1 salt solution with salt concentration c_∞ contains both cations and anions at that concentration, and both ions must be counted. The ion's charge does not play a role in calculating the entropy of desalination.

2.2.2. Extensions for non-ideal solutions

We will discuss various simplifications in a later section, but let us first briefly point out how additional energy terms can be included. A first effect is that of electrostatic Coulomb interactions between ions, which for a 1:1 salt can be described by the modified Bjerrum equation [12]

$$f_{elec} = -\frac{3}{2} k_B T \, \lambda_B \, n_\infty^{4/3} \tag{7}$$

where f_{elec} is the contribution to the free energy density of a solution. This contribution, f_{elec}, can be evaluated for each of the three streams, and then multiplied by the respective volume flow rate, ϕ_v, and all terms are added to $e_{\min}$ (with an additional minus-sign for the feed stream). The salt concentration in numbers per volume, n_∞, relates to salt concentration c_∞ in moles per volume according to $n_\infty = N_{av} c_\infty$, where N_{av} is Avogadro's number. Furthermore, λ_B is the Bjerrum length which in water at room temperature is around $\lambda_B \sim 0.72$ nm, and k_B is Boltzmann's constant. We can rewrite Eq. (7) to

$$f_{elec} = -\alpha \, c_\infty^{4/3} \tag{8}$$

where at room temperature the prefactor is $\alpha \sim 225$ J·m/mol$^{4/3}$. For salt mixtures other than 1:1 salts, numerical analysis of the modified Bjerrum theory is required [12].

Another contribution to the energy is an ion volume (size) effect that shows up at higher concentrations, which describes that the (hydrated) ions cannot overlap, i.e., they exclude space for one another. The Carnahan–Starling equation of state can be used to describe this effect (when we assume that all ions have the same hydrated size and all are more or less spherical), and this leads to a further contribution to the free energy, thus to $e_{\min}$. For each flow this contribution is [13]

$$\frac{f_{vol}}{RT c_{tot}} = \frac{4\phi - 3\phi^2}{(1-\phi)^2} = 4\phi + 5\phi^2 + 6\phi^3 + \cdots \tag{9}$$

where c_{tot} is the total ion concentration (for a $z{:}z$ salt, $c_{tot} = 2c_\infty$) and ϕ is the volume fraction of all ions together, i.e., $\phi = c_{tot} v_i$, where v_i is the molar volume of an ion (all ions are assumed to have the same volume.). The contribution f_{vol} can be multiplied by ϕ_v and added to $e_{\min}$. As a numerical example, for a 1:1 salt at $c_\infty = 525$ mM, with ions of a hydrated size of $\sigma = 0.5$ nm (size is twice the radius), the ion volume fraction is $\phi = 0.0414$. With the electrostatic and volumetric contributions implemented, then for the previous numerical example, the minimum energy consumption increases from $E_{\min} = 1.00$ kWh/m^3 to $E_{\min} = 1.14$ kWh/m^3. Further extensions relate to the energies of ion–ion association and ion (de-)protonation [14], but we do not discuss these effects in this review.

2.2.3. Simplifications of the thermodynamic expressions

Various simplifications are possible to the above general expressions for the theoretical minimum energy. Here we consider a symmetric $z{:}z$ salt solution, with one type of cation and one type of anion. We only discuss the ideal, entropic, contribution. We present results for the energy per m^3 of permeate (diluate, freshwater) produced. Each of the three streams, feed, permeate and concentrate, is described by a certain value for the salt concentration c_j.

A first simplification relates to RO in the limit of very low WR and very low c_p. In this limit, on the feed side the concentration does not change along the module. We only produce a very low volume of totally clean freshwater. We now obtain the result that the minimum energy per volume of freshwater is given by

$$E_{\min} = \Pi_f \tag{10}$$

where Π_f is the osmotic pressure of the feed solution. The osmotic pressure for ideal conditions is given by $\Pi = RT \sum_i c_i$, and thus for a $z{:}z$ salt, $\Pi = 2RT c_\infty$.

In general, for a perfectly selective membrane, and thus $\Pi_p = 0$, the hydrostatic pressure difference that must be applied across the membrane in a pressure-driven process, $\Delta P^{h,\infty}$, must be larger than $\Pi_{dbl/mem}$, where $\Pi_{dbl/mem}$ is the osmotic pressure at the interface between the diffusion boundary layer (DBL) and membrane, and this osmotic pressure is larger than Π_f by the over-pressurization factor, α_1. This effect is commonly called concentration polarization (CP). The factor α_1 can be close to unity, when CP is negligible, which will be the case for a low permeate flux and high enough crossflow of water (water flow along the membrane), but values of $\alpha_1 = 1.5$ or larger are also possible. The hydrostatic pressure is typically larger than $\Pi_{dbl/mem}$ by a second factor, α_2, again larger than 1, to have transmembrane water flow. Thus, in this simplest analysis of a perfectly selective membrane at WR $\to 0$, the energy efficiency of an RO membrane is given by

$$\eta_{RO} = \frac{\Pi_f}{\Delta P^{h,\infty}} = \frac{1}{\alpha_1 \alpha_2}. \tag{11}$$

In a more general case, combining the various balances with the expressions for S_i, we obtain for E_{min}, now for arbitrary values of WR and c_p, for a $z{:}z$ salt of one anion and one cation, the result that [15]

$$\frac{E_{min}}{2RT} = \frac{c_f}{WR} \ln \frac{c_c}{c_f} - c_p \ln \frac{c_c}{c_p} \tag{12}$$

where all concentrations c_i are salt concentrations in mol/m^3. When c_p approaches zero, i.e., complete salt removal, then Eq. (12) simplifies to [15]

$$\frac{E_{min}}{2 c_f RT} = -\frac{\ln(1 - WR)}{WR} = 1 + \frac{1}{2} WR + \frac{1}{3} WR^2 + \cdots \tag{13}$$

which in the limit of WR $\to 0$ simplifies to Eq. (10). Note that if we apply these equations to a solution containing a single neutral solute, not a 1:1 salt, then factors '2' on the left side of Eqs. (12) and (13) must be omitted.

It is very important to note that Eqs. (10) and (13) are only correct when $c_p \to 0$. For non-zero values of c_p, this energy, in the limit of WR $\to 0$, is given by

$$E_{min}/2RT = c_f - c_p - c_p \ln \frac{c_f}{c_p}. \tag{14}$$

2.3. Practical energy use in RO and ED

In the above section the thermodynamic, minimum, energy of a desalination process was discussed. But what is the actual, real, or practical, energy consumption? The main factors are the pressure required to pump fluid through channels, and in RO to press water through the membrane, while in ED we need energy to generate a flow of electrical current across the ED stack.

The energy required to pressurize a stream is ΔP^h times flowrate $\phi_{v,j}$, which is a number with unit J/s = W. This is the energy to pump feedwater into a module. And to pump water exiting one module into the next operating at a higher pressure. At the end of a train of modules, it is possible to install an energy recovery device (ERD). If the water on the retentate side (the concentrate; a smaller volume than the flow of feedwater) passes an ERD, exiting at atmospheric pressure, an energy can be recovered equal to $\eta_{ERD} \cdot \Delta P^h \cdot \phi_{v,c}$, with η_{ERD} the energy efficiency of the ERD.

Another practical limitation, even for ideal operation, is that we generally have a limited number of modules. In RO with a single module, for a membrane that perfectly retains all solutes, the minimum pressure is given by the retentate (concentrate) concentration, which in this case for perfect retention relates to c_f by $c_c = c_f / (1 - WR)$. So the minimum energy per unit permeate, practically, cannot be less than

$E_{min,prac} = RT c_f / (1 - WR)$ [15], and with E_{min} given by Eq. (13), this implies a practical single stage RO efficiency of

$$\eta_{RO} = \frac{1 - WR}{WR} \cdot \ln(1 - WR) = 1 - \frac{1}{2} \cdot WR - \frac{1}{6} \cdot WR^2 - \cdots \tag{15}$$

which can be multiplied by $1/\alpha_1 \alpha_2$.

In ED also some energy is required to push water through tubings and channels of the ED stack, but this is low compared to the main energy input, which is electricity for running current across the stack. For a certain current I (in A, i.e., Ampère), and cell pair voltage V_{cp}, then for each cell pair the electrical energy input is $I \cdot V_{cp}$ (unit J/s = W), and with N cell pairs in an ED stack, this energy is multiplied by N to obtain the electrical energy input for the stack. Inside each cell pair the voltage V_{cp} is due to resistances for current to cross the diluate and concentrate channels, to cross the membranes, and due to the Donnan voltages at the membrane–solution edges. These Donnan voltages are not a resistance (they are not a direct function of the current), but are a consequence of the thermodynamics of desalination, i.e., the Donnan voltage cannot be reduced to zero by running at low currents. Of the Ohmic resistances, the largest loss is in the low-salinity diluate channel. In EDI this resistance is reduced with ion-exchange resin material in these channels. In an ED stack (of 10s or 100s of cell pairs) there are also two end-compartments in which electronic current transfers to ionic current, and vice-versa. There is a voltage loss associated with the Faradaic reactions there, but with increasing numbers N of cell pairs, this voltage loss (of the order of the voltage over 1 cell pair) becomes inconsequential for the energy requirements of a full ED stack. In ED generally only a single value of the cell pair voltage is applied to the stack as a whole, which also leads to a practical limit in the energy efficiency, which is discussed in Section 4.

The energy thus invested in RO and ED by pressure and electricity (including energy recovery), is always larger than the thermodynamic energy as calculated in Section 2.2. Thus, the ratio of thermodynamic energy e_{min} over the real, or practical energy, i.e., the energy efficiency η, is always less than unity, i.e., we always have $\eta < 1$.

3. One- and two-dimensional models for RO with neutral solutes

3.1. Flowrates and retention in a 1D model of RO for neutral solutes

Reverse osmosis (RO) is a process to remove solutes from water by pushing water through a membrane which largely blocks passage for solutes. This is the general mechanism of all pressure-driven membrane processes, but for water desalination the size of the pores (free volume) in the membrane must be very small, typically well below 1 nm in the selective toplayer of an RO membrane. In classical literature, RO is called hyperfiltration, but nowadays this term has been replaced by RO. Nanofiltration (NF) is similar to RO but has slightly larger pores, and thus the applied hydrostatic pressure is lower, with the retention of monovalent ions significantly reduced. NF is therefore considered to be suitable for the selective separation of divalent ions and other larger molecules from monovalent ions.

Because RO (and NF) can be used not only to desalinate water but also to remove other (larger) molecules that may not necessarily be charged, it is useful to start with theory for uncharged solutes. A key parameter is the permeate water flux, v_w, also called transmembrane water velocity [5]. This is the flux, or velocity, of water in the direction across the membrane. For uncharged solutes, if v_w is known, and if there are no special interactions between the solutes, then, interestingly all solutes can be treated separately, and their transport rates are not coupled. This is also why equations that we derive below for the retention of neutral solutes in RO are independent of feed solute concentration, as long as v_w is set to a certain value. If v_w is not fixed, but instead the applied pressure is set to a certain value, then this is not the case but via the osmotic pressure the concentration feeds back into the transport problem and into the (prediction of) retention. Note that this situation is very different for electrolyte solutions (i.e., a

solution containing ions), because then an electric field develops to ensure that the electrical current is zero, and this always leads to various couplings between the ion fluxes. RO for electrolytes will be discussed in Section 6.

Based on the solution-friction model, see Section 5, we can derive for the flux of neutral species across a porous membrane (see Eqs. (1), (18), and (19) in Ref. [16])

$$J_i = K_{f,i}\, c_{m,i}\, v_w - K_{f,i}\, D_{m,i}\, \frac{\partial c_{m,i}}{\partial x} \tag{16}$$

where the transmembrane solute flux J_i and water flux v_w are defined per unit geometric membrane area, thus they are superficial velocities, i.e., they are not pore-based, interstitial, velocities. Concentrations are defined per unit volume of the water-filled pores in the membrane. Eq. (16) includes transport due to a solute concentration gradient (second term), and due to solute advection, which is the movement of solutes because they 'flow along', i.e., are advecting with, the water that flows through the membrane (first term).[2] Here, x is the coordinate axis directed across the membrane. The diffusional term depends on a membrane-based diffusion coefficient, $D_{m,i}$, which includes the effects of porosity and tortuosity. Eq. (16) follows as a simplification of the two-fluid model (TFM) that will be explained in Section 5. The friction factor $K_{f,i}$ depends on the extent of solute–membrane friction, and thus relates to membrane pore size and the (hydrated) size of the solutes. In the absence of solute–membrane friction, the solutes move freely with the fluid (i.e., with the water in the pores), while they are still subject to diffusional forces (and electrical forces when charged), and in that case $K_{f,i} = 1$.

Now, for RO, a value of $K_{f,i} = 1$ is unlikely, because that would mean zero solute–membrane friction, and thus we expect $K_{f,i}$ to be less than unity. However, it is not likely that we have $K_{f,i} = 0$, in which case not only the advection term cancels (which would lead to the solution–diffusion model that we discuss later on), but then there is no diffusional transport of solutes either, and such a membrane would therefore perfectly block solutes under all conditions. This is not the case in a real RO or NF membrane, with solutes still passing the membrane, and thus it must be the case that $K_{f,i}$ is larger than zero. Thus, in an RO membrane with neutral solutes, diffusion and advection are to be considered jointly, as described by Eq. (16), and it is incorrect to neglect advection altogether.

Before continuing with a discussion of transport models, we must first introduce two other model elements. First, the solute concentration just in the membrane is related to that just outside. To that end we make use of a partitioning equation [17,18], which follows from chemical equilibrium of a species i across an interface, which applies on both outer surfaces of a membrane [5], resulting for neutral solutes in

$$\Phi_i = S_i = \frac{c_{m,i}}{c_{\infty,i}} \tag{17}$$

where index ∞ refers to a position just outside the membrane. For RO with ions, see sections 5.2 and 6.2, an additional Donnan effect arises, which in this paper we treat separately, i.e., do not include in S_i or Φ_i. The partitioning coefficient, Φ_i, is the same as the solubility of a species in a material, S_i, and this term is for instance due the chemical affinity of a solute with a certain phase (medium) relative to its affinity with another phase, but also other effects of solute–membrane interaction can be absorbed in Φ_i [17]. In RO with neutral solutes, we always have $\Phi_i < 1$ or $K_{f,i} < 1$, or both.

A further element in RO modeling is the 'permeate equation', an equation essential to describe RO in a one-dimensional (1D) geometry,

valid when there is no flow along the membrane on the permeate side, which is Eq. (8) in Ref. [5], and Eq. (24) in Ref. [19]

$$c_{p,i} = \frac{J_i}{v_w} \tag{18}$$

which looks very simple, but is actually a quite intriguing result. It states that the concentration of solutes on the permeate side is a direct function of the ratio of solute flux through the membrane over the water flux. This is a correct result in steady-state, thus with conditions on the upstream side unvarying in time. It is also valid when on the upstream side conditions change in time and the permeate is regularly removed; as a consequence water that permeated the membrane at earlier moments does not mix up with fresh permeate. In a complete (2D) module, Eq. (18) can also be used with average values of J_i and v_w (averaged over the complete module).

Let us first discuss the well-known solution–diffusion (SD) model. In the SD-model, the advection term in Eq. (16) is set to zero and thus only diffusion drives solutes across the membrane [20]. We can then integrate Eq. (16) on the basis of the fact that in steady-state the molar flux of solutes, J_i, is constant across the membrane, and after combination with Eq. (17), we arrive at

$$J_i = k_{m,i} K_{f,i} \Phi_i \left(c_{f,i} - c_{p,i} \right) \tag{19}$$

where the membrane mass transfer coefficient, $k_{m,i}$, is $k_{m,i} = D_{m,i}/L_m$, with L_m membrane thickness. The abbreviation SD refers to the combination of a solution process (described by the Φ_i-term) and solute diffusion across the membrane, of which the rate is described by $k_{m,i} K_{f,i}$. In this SD-model, the flow of solutes, and that of the solvent, 'are completely independent without any effect of one on the other when, in general, they may be coupled by either frictional or convective effects' [21]. Combining Eqs. (18) and (19) leads to an expression for retention R_i in the SD-model given by

$$R_i = \frac{Pe_i}{Pe_i + K_{f,i} \Phi_i} = \frac{v_w}{v_w + \omega} \tag{20}$$

where the membrane Péclet-number is given by $Pe_i = v_w/k_{m,i}$ and ω is a factor we discuss further on. Eq. (20) predicts that if we steadily increase the permeate water flux v_w, thus Pe_i, at some point we always reach a retention as close to 100% as desired [22], at least as long as CP-effects can be avoided.

When we do not make the SD assumption, we can solve Eq. (16) including advection as well. Calculation results stemming from this model are presented in Fig. 3. With the same assumptions as before, integration of Eq. (16) across the membrane results in

$$J_i = K_{f,i}\, v_w\, \frac{c_{m,L,i} \exp\left(Pe_i\right) - c_{m,R,i}}{\exp\left(Pe_i\right) - 1} \tag{21}$$

where subscripts L and R refer to the left and right sides of the membrane, at positions just inside the membrane. We associate 'left' with the feed/retentate side, for which we index 'f', and associate 'right' with the permeate side (freshwater, diluate), with index 'p'. Eq. (21) is sometimes referred to as the Hertz equation [23]. We combine Eqs. (17) and (21), which leads to

$$\begin{aligned} J_i &= K_{f,i}\, \Phi_i\, v_w\, \frac{c_{f,i} \exp\left(Pe_i\right) - c_{p,i}}{\exp\left(Pe_i\right) - 1} \\ &= K_{f,i}\, \Phi_i\, v_w \sqrt{c_{f,i} c_{p,i}}\, \frac{\sinh\left(1/2 \left(Pe_i + \ln\left(c_{f,i}/c_{p,i}\right)\right)\right)}{\sinh\left(1/2\, Pe_i\right)} \end{aligned} \tag{22}$$

which is the general result for retention in an RO membrane with neutral solutes (e.g., Eq. (10) in Ref. [24]). Because of the dependence of solubility, i.e., partitioning, described by the factor Φ_i, in combination with a derivation based on ion–water and ion–membrane friction, captured by the factor $K_{f,i}$, we call this the solution-friction model, or SF-model. It is identical to the sieving model put forward by Kedem and colleagues in the 1950s and 1960s [19,25], though there are differences in the derivation. The same set of expressions is also called

---

[2] Advection was just explained and is different from convection, which is the flow of a continuum fluid because of pressure gradients.

the homogeneous model for RO membranes [5]. The sieving coefficient, σ_i, is a common term in the literature on this subject and relates to $K_{f,i}$ and Φ_i according to

$$\sigma_i = 1 - K_{f,i}\Phi_i. \tag{23}$$

This result was already arrived at by Spiegler and Kedem, see their Eq. (49) in case in their equation we implement that $v_s \ll v_w$, see also Eq. (76) in Ref. [26], or Eq. (16) in Ref. [27]. We combine Eqs. (2), (18), and (22) to obtain for solute retention

$$R_i = \frac{(1 - F)\,\sigma_i}{1 - F\,\sigma_i} \tag{24}$$

where $F = \exp(-Pe_i)$. Eq. (24) is equivalent to Eq. (3) in Ref. [27], Eq. (4) in Ref. [16], Eq. (38) in Ref. [3], and Eq. (129) in Ref. [28], when we make the following conversions: $\omega = (1 - \sigma_i)\,k_{m,i}$, $P = P_s = K_f\Phi_i k_{m,i}$, and thus $k_{m,i} = P_s/(1 - \sigma_i)$. Another formulation is $(1 - \sigma_i)/P_s \cdot v_w = \ln\{c_p \cdot \sigma_i/(c_p - c_f(1 - \sigma_i))\}$ (Eq. (9) in Ref. [29]). Note that when a DBL or CP layer is included, we must replace here c_f for the concentration right at the membrane. Note also that these equations are only valid in the limit of a low water recovery, and assume that we describe transport of neutral solutes.

For low v_w, the expression for solute flux J_i, Eq. (22), simplifies to (see Eq. (3.1) in Ref. [25])

$$J_i = (1 - \sigma_i)\left(k_{m,i}(c_{f,i} - c_{p,i}) + \langle c_i \rangle v_w\right) \tag{25}$$

where $\langle c_i \rangle$ is the average of $c_{f,i}$ and $c_{p,i}$. Eq. (25) is called the arithmetic mean expression [23]. Based on Eq. (24), retention in the limit of low v_w is given by

$$R_i = \frac{\sigma_i}{1 - \sigma_i}\,Pe_i = \frac{\sigma_i}{\omega}\,v_w \tag{26}$$

which shows that for very low water velocities, retention goes to zero, and for a non-zero retention we need $\sigma_i > 0$ and thus we need either a non-unity $K_{f,i}$-factor or a non-unity partitioning function, Φ_i. Note that Eq. (26) is not the same as Eq. (20) which describes retention according to the SD model. Note as well that Eq. (26) does not follow from combining Eqs. (2), (18) and (25).

In the other limit, of a high permeate water flux, v_w, Eq. (22) simplifies to

$$J_i = (1 - \sigma_i)\,c_{f,i}\,v_w \tag{27}$$

which implies that in this limit solute flux is only due to advection, and no longer depends on diffusion. In this high-Pe limit, retention is given by

$$R_i = \sigma_i \tag{28}$$

which is Eq. (30) in Ref. [19] and Eq. (34) in Ref. [28]. Eq. (28) describes that an RO membrane has a natural limit in what retention it can achieve, determined by the extent to which solutes are excluded from the membrane (which implies a value of $\Phi_i < 1$), and by the extent of solute–membrane friction (which leads to $K_{f,i} < 1$). If a membrane does not do either, i.e., it does not exclude solutes, i.e., $\Phi_i = 1$, and it does not impose a frictional force on solutes at all, i.e., $K_{f,i} = 1$, then the SF theory predicts that retention will be zero, and in our view that is a correct result: for an RO membrane to function, either solutes must be excluded from the membrane, leading to $\Phi_i < 1$, or there must be a solute–membrane friction, i.e., $K_{f,i} < 1$, and ideally both. Instead, the SD-model, Eq. (20), does not make these detailed predictions at all, see a similar discussion in Ref. [21].

Interesting is the effect of membrane thickness, which influences $k_{m,i}$. In the limit of a high permeate water flux, v_w, there is no effect of thickness on retention, though there is for lower values of v_w. In that case a thicker membrane leads for the same v_w to a higher retention. Or vice-versa, when for the same v_w the membrane is made thinner, thus Pe_i decreases, then retention decreases, because diffusion of solutes increases, see Fig. 3A. Thus, thin(ner) membranes are not necessarily advantageous.

3.2. A 1D model for RO of neutral solutes including concentration polarization

Next we extend the SF-model with solute transport across a diffusion boundary layer (DBL), or alternatively called concentration polarization layer (CP layer) located in front of the membrane, i.e., on the upstream side [30]. This layer is assumed to have a certain thickness and all water and solutes are transported across this layer before reaching the membrane. Eq. (21) which describes solute advection and diffusion in a membrane also applies to the DBL, now with $K_{f,i} = 1$ because there is no porous structure in the DBL that generates friction with the solutes. Furthermore, $c_{m,L,i} \rightarrow c_{f,i}$, $c_{m,R,i} \rightarrow c_{int,i}$, and $Pe_i \rightarrow Pe_{dbl,i}$. We then arrive at

$$
\begin{aligned}
J_i &= v_w\,\frac{c_{f,i}\exp(Pe_{dbl,i}) - c_{int,i}}{\exp(Pe_{dbl,i}) - 1} \\
&= v_w\sqrt{c_{f,i}c_{int,i}}\,\frac{\sinh\left(1/2\left(Pe_{dbl,i} + \ln(c_{f,i}/c_{int,i})\right)\right)}{\sinh\left(1/2\,Pe_{dbl,i}\right)}
\end{aligned} \tag{29}
$$

where $Pe_{dbl,i} = v_w/k_{dbl,i}$, with $k_{dbl,i} = \varepsilon_s D_{\infty,i}/L_{dbl}$, where ε_s is a porosity- and tortuosity-correction in the solution phase, e.g., because of a spacer material, and where L_{dbl} is an estimated thickness of the DBL layer. With more stirring, or a higher cross flow rate (velocity of the water pumped along the membrane), this thickness goes down and $k_{dbl,i}$ goes up. In Eq. (29) we use 'f' for feed, but that is only correct in an experiment at very low water recovery. More generally, when we use this equation in a 2D module calculation, we should use here 'u, b' for the bulk phase on the upstream side, instead of 'f'. The concentration at the interface between DBL and membrane (but still in solution) is $c_{int,i}$. In the limit of a low water flow rate, v_w, Eq. (29) simplifies to

$$J_i = k_{dbl,i}(c_{f,i} - c_{int,i}) + 1/2\,v_w(c_{f,i} + c_{int,i}). \tag{30}$$

In a 1D geometry where Eq. (18) applies, Eq. (29) can be rewritten to

$$c_{int,i} = c_{p,i} + (c_{f,i} - c_{p,i})\exp(Pe_{dbl,i}) \tag{31}$$

and if $c_{int,i} \gg c_{p,i}$, then Eq. (31) simplifies to $c_{int,i} = c_{f,i} \cdot \exp(Pe_{dbl,i})$. For any asymmetric binary salt, Eqs. (29)–(31) also apply, but the diffusion coefficient $D_{\infty,i}$ is replaced by the harmonic mean diffusion coefficient of the binary salt, D_{hm}, see Ref. [12].

When we combine all these equations, we obtain the following generalized RO solute retention equation that includes the effect of concentration polarization (Eq. (13) in Ref. [5])

$$R_i = 1 - \left[1 + \left((1 - \sigma_i)^{-1} - 1\right)\cdot\exp(-Pe_{dbl,i})\left(1 - \exp(-Pe_i)\right)\right]^{-1}. \tag{32}$$

When $Pe_{dbl,i} \rightarrow 0$, i.e., when the mass transfer coefficient of the DBL is large enough, for instance because of sufficient stirring, then Eq. (32) simplifies to Eq. (24). Eq. (32) predicts a maximum in retention, as also shown in Fig. 3A, and this maximum retention is at a membrane Pe-number given by $Pe_i = \ln(1 + w)$ where $w = k_{dbl,i}/k_{m,i}$ (Eq. (15) in Ref. [5]). The maximum retention is then given by $R_{max,i} = 1 - \left[1 + \left((1 - \sigma_i)^{-1} - 1\right)\cdot w \cdot (1 + w)^{-(1 + 1/w)}\right]^{-1}$ (Eq. (15') in Ref. [5]), which for $w \rightarrow \infty$ simplifies to Eq. (28). For reference, we give the result when the SD-model is combined with a CP-layer based on Eq. (31), for a 1D geometry, which is $R_i = v_w/(v_w + \omega\exp(Pe_{dbl}))$.

In the general case of the SF-model in combination with a CP-layer, based on Eq. (32), we can analytically solve all relevant properties in and near the membrane as follows. For a known value of v_w, retention R_i follows from Eq. (32), then Eq. (2) leads to $c_{p,i}$, J_i follows from Eq. (18), Eq. (31) results in the concentration just on the upstream outside side of the membrane, and then with Eq. (17) we obtain the solute concentration just inside the membrane on that same side. Subsequently we can use Eq. (35), which we will discuss further on, to calculate the applied pressure. If the applied pressure is an input parameter, then an extra iteration is needed, but that is not complicated.
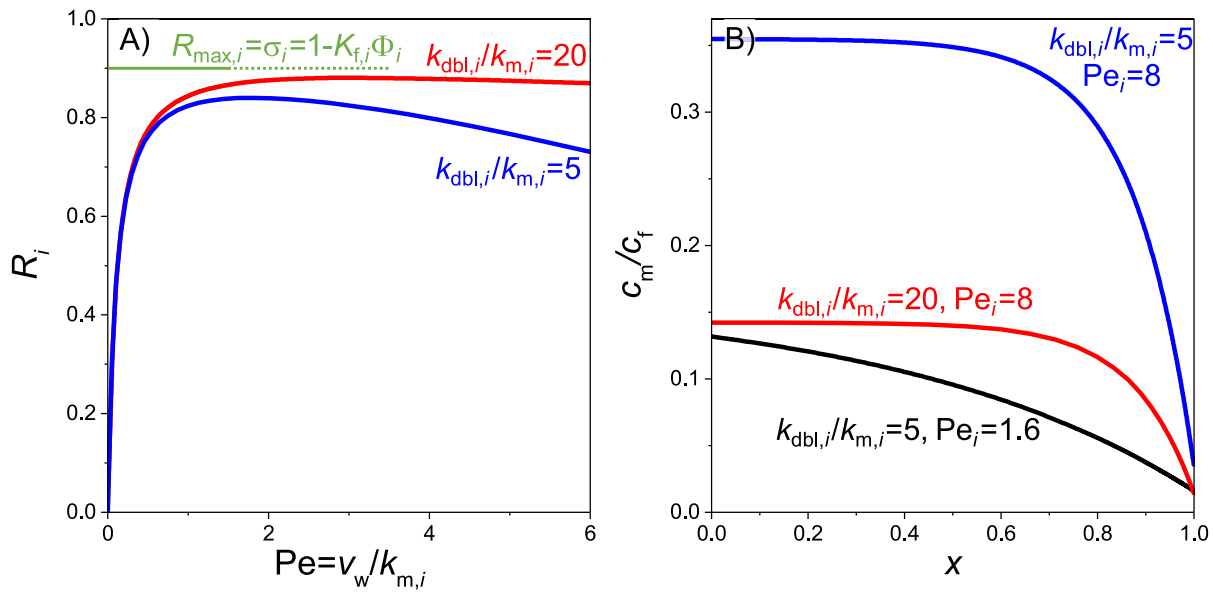
Fig. 3. Results of calculations for retention of neutral solutes by an RO membrane in a 1D geometry, combining membrane transport modeling with solute partitioning and concentration polarization, based on Eqs. (24) and (28). (A) Retention as function of permeate water flux, v_w, and solute mass transfer coefficients ($\sigma_i = 0.9$). (B) Examples of solute concentration profiles across the membrane.

We present in Fig. 3A results for retention as described by Eq. (32) for various values of the ratio $k_{dbl,i}/k_{m,i}$. Also results are presented for the limiting retention given by Eq. (28). For selected conditions, concentration profiles are presented in Fig. 3B. These profiles are quite strongly non-linear with a steeper decay in concentration near the permeate side. They are not straight lines as would be expected in the SD model.

3.3. Pressure and water flow in a 1D model of RO for neutral solutes

Having discussed how solutes are retained by RO membranes, we next describe the relation between the hydrostatic pressure that is applied across an RO membrane, $\Delta P^{h,\infty}$, and the resulting permeate water flux, v_w. The force balance on the water that will be presented in Section 5 describes fluid flow through porous media in the presence of solutes that move through that same porous structure. The theory describes how water flows because of gradients in hydrostatic and osmotic pressure [31] (the latter due to gradients in total solute concentration), and is slowed down by friction with the membrane matrix and by friction with solutes. When solutes also have friction with the membrane (resulting in $K_{f,i} < 1$), then the water velocity decreases: with increasing solute–membrane friction, solutes become more of an obstacle for water to flow. In the opposite limit when solutes 'just flow along' with the water, without solute–membrane friction, they do not hinder water transport and then this same theory leads for neutral solutes to the classical Darcy equation for fluid flow through a porous medium. At the edges of the membrane, we have jumps both in osmotic pressure and hydrostatic pressure [28,32,33], and it is essential to understand these to predict the direction of water flow, especially in the absence of a significant hydrostatic pressure. These topics are addressed in Sections 5 and 6.

Interesting are the changes of pressure across the CP-layer, i.e., across the DBL. The osmotic pressure increases through the DBL, because it is a direct function of the local solute concentration, which also increases towards the membrane (because the solutes are rejected by the membrane while water flows through). At the same time, the hydrostatic pressure does not change through the DBL, i.e., the externally applied hydrostatic pressure 'arrives at' the membrane unchanged. Only there, at the outer surface of the membrane, are there jumps in the hydrostatic pressure and osmotic pressure upon entering the membrane [33–36].

The physical phenomena at the outsides of the membrane are highly intriguing, even for neutral solutes. We know there is a jump 'down' in solute concentration upon entering the membrane when solutes are excluded from the membrane, described by $\Phi_i < 1$. A first question is then how the osmotic pressure changes across the interface. The correct analysis leads to the result that also the osmotic pressure goes down, from a value Π^∞ just outside the membrane to a value Π^m just inside the membrane, with $\Pi^m < \Pi^\infty$ when $\Phi_i < 1$ for all solutes. For ideal solutions the osmotic pressure (both inside and outside a membrane) is proportional to the solute concentration according to $\Pi = c\,RT$ (where c is a total concentration, i.e., a summation over all solutes), and thus the jump in osmotic pressure (counted in the membrane relative to outside) is $\Delta\Pi = (c_{T,m} - c_\infty)\,RT$, where $c_{T,m}$ is a total solute concentration in the membrane. If we now include the partitioning equation we arrive at $\Delta\Pi = -c_\infty(1 - \Phi_i)\,RT$ (assuming that all solutes have the same Φ_i), which is negative. This means the osmotic pressure goes down upon entry into the membrane. The magnitude of this change is proportional to the solute concentration just outside the membrane, and thus $\Delta\Pi$ can be quite significant on the upstream side of a membrane, while on the downstream side there will hardly be any jump in pressure between outside and inside the membrane.

The next step is to find the relationship between this osmotic pressure change at the membrane interface and the hydrostatic pressure change there. The result is very elegant, and follows from analysis of mechanical equilibrium across this interface, namely that the *total* pressure is invariant across each of the membrane interfaces (between just outside and just inside) [37], with this total pressure a summation of hydrostatic pressure and *minus* the osmotic pressure. This will be further explained in Section 5 as the consequence of a force balance acting on the water evaluated over a very thin layer with steep changes in pressures, similar to how electrical double layer theory follows from chemical equilibrium across an interface with an associated change in voltage. Thus, at each of the two membrane interfaces we have

$$\Pi^m - \Pi^\infty = P^{h,m} - P^{h,\infty} \tag{33}$$

where '∞' refers to just outside the membrane, and 'm' to just inside. Thus, a step downward in osmotic pressure upon entry into the membrane (in case $\Phi_i < 1$) translates into an equally large step downward in hydrostatic pressure (Eq. (60a) in Ref. [26]). This step downward is

the most significant on the side of the membrane with a large solute concentration. Note that in the SD-model it is stated that only on the downstream side of the membrane there is a pressure drop, with no pressure change on the upstream side of the membrane, see for instance a discussion and references in Ref. [21]. However, for RO with neutral solutes, these assumptions do not agree with an analysis based on mechanical equilibrium.

Inside the membrane, the velocity of water follows from a friction balance that we explain in Section 5, which in a general form is Eq. (84). For neutral solutes, this becomes

$$v_w = -\Bbbk_{F\text{-}m}^{\dagger} \left(\frac{1}{RT} \frac{\partial P^{h,m}}{\partial x} - \left(1 - K_{f,i}\right) \frac{\partial c_{T,m}}{\partial x} \right) \tag{34}$$

where we assume for all solutes the same $K_{f,i}$. Here $\Bbbk_{F\text{-}m}^{\dagger}$ is a water–membrane permeability that also includes friction of water with the membrane via a friction of solutes with the membrane. This latter effect disappears when $K_{f,i} = 1$ and then the †-index can be dropped. In that case we will have a linear pressure gradient in the membrane that leads to transmembrane water flow (Eq. (65) in Ref. [26]). Assuming a constant value for $\Bbbk_{F\text{-}m}^{\dagger}$, we can integrate over the membrane thickness, L_m, implement Eq. (33) for mechanical equilibrium, as well as the relation for solute partitioning, and then obtain the classical result that the transmembrane water flow rate is given by

$$v_w = k_{F\text{-}m}^{\dagger} \left(\Delta P^{h,\infty} - \sigma_i \cdot \Delta \Pi^{\infty} \right) (RT)^{-1} \tag{35}$$

where Δ's here and in the remainder of this section refer to a value upstream minus that downstream. Eq. (35) is Eq. (41) in Ref. [34], and is Eq. (10.21) in Ref. [38]. (Note that in the SD-model, see Eq. (12) in Ref. [20], the term σ_i is not present.) Interestingly, Eq. (35) describes that for water to flow, the applied pressure must compensate the osmotic pressure *difference* across the membrane (not overcome 'the' osmotic pressure at the DBL/membrane interface), and the less so the lower σ_i. Thus if solutes are not very much excluded by the membrane, water will still flow while the hydrostatic pressure can be much lower than the upstream osmotic pressure [3]. Note that ∞ here refers to just outside the membrane, so on the upstream side ∞ refers to a position between DBL and membrane.

In Fig. 4A, we analyze the required transmembrane pressure for any value of the water flux, v_w, and we notice that for each flux there is one pressure. It is not the case that we first need to overcome some discrete value of the osmotic pressure of the feedwater before water starts to flow across the membrane. This is because the osmotic pressure that must be overcome is the *difference* in osmotic pressure across the membrane, and retention is low at low water velocities, and then the osmotic pressure on the permeate side approaches that on the feed side, i.e., in the limit of very low transmembrane water velocities, the osmotic pressure difference goes to zero. However, as also shown in Fig. 4A, the more a membrane becomes selective, with the reflection coefficient increasing, in this case from $\sigma_i = 0.90$ to $\sigma_i = 0.98$, the more we obtain a curve in alignment with the common understanding that a minimum pressure is needed to overcome the osmotic pressure, before water starts to flow. Furthermore, Fig. 4B illustrates that in the SF model the flow of solutes more or less monotonically increases with pressure. This is very different from what the SD-model predicts, that solute flow is independent of pressure [22].

3.4. Energy efficiency of RO with neutral solutes in 1D geometry

Having analyzed the flow of solutes and water as function of pressure, we can next analyze energy efficiency, η_{RO}, for which results are presented in Fig. 5. To calculate the energy efficiency, we must divide the 'thermodynamic' energy, given by Eq. (14), by the real input energy, which is the pressure difference $\Delta P^{h,\infty}$ times the flow of water across the membrane, $\phi_{v,prod}$ (which is equal to the water flowrate v_w times membrane area). When we take the ratio of these two energies, water flowrate cancels out, and we obtain $\eta_{RO} = E_{min}/\Delta P^{h,\infty}$.

This efficiency η_{RO} starts at zero at very low water velocities (for low Pe_i), and then increases. In the limit of a very high water–membrane permeability ($\beta \to \infty$, with $\beta = k_{F\text{-}m}^{\dagger} \Pi_f / \left(RT k_{m,i} \right)$, where the osmotic pressure of the feed stream is $\Pi_f = c_f RT$), and in the absence of concentration polarization (CP), we can reach an energy efficiency of around 80% when $\sigma_i = 0.90$, which is a maximum value that cannot be further increased at that value of σ_i. When the CP layer plays a more important role, we need a higher pressure at the DBL/membrane interface to overcome the higher osmotic pressure, and this reduces η_{RO}. And when the water–membrane permeability decreases, efficiency also drops, for instance to values around 40%–50% at $\beta = 10$, see Fig. 5.

Interestingly, this parameter β does not depend on membrane thickness, so the equations do not simply predict that we have a higher energy efficiency if we reduce membrane thickness. The only effect of thickness is via $k_{m,i}$ which is part of the definition of Pe_i. A thinner membrane leads to lower Pe_i, and can help to increase efficiency (see curve for $\beta = 10$ when we go from high Pe_i back to $Pe_i \sim 0.4$), but for Pe_i already small, a thinner membrane only reduces efficiency because the membrane becomes more leaky and retention goes down which reduces E_{min} and that reduces η_{RO}. This illustrates that – even in this relatively simple example of RO of a neutral solute in a 1D geometry for low water recovery – the effect of various parameters is not always straightforward. An extended calculation for a full module that we discuss next demonstrates that the relations between water recovery, retention, and energy efficiency can be even more intricate.

3.5. 2D model for an RO module for neutral solutes

In the present section we theoretically analyze an RO module for the removal of neutral solutes. The model uses analytical expressions for solute and water flow across the membrane at any position in the module, while solving mass balances in the direction between inlet and outlet of a flow channel, i.e., in the z-direction along the membrane, see Fig. 6A. So we call this a two-dimensional (2D) model, because that is the physical geometry that is described. The two coordinate axes z on each side of the membrane are parallel, and we assume the water to flow co-currently, i.e., the exits of both channels are on the same end of the module. On each side of the membrane we assume one value for the pressure, i.e., we neglect pressure changes through the flow channels, that is, along the membrane. Thus, in the entire module there is one value of $\Delta P^{h,\infty}$. On the permeate side there is no inlet, but all water that passes the membrane, going from feed to permeate, leaves as the permeate product stream.[3] We now introduce a dimensionless coordinate axis along the membrane, ξ, which starts at $\xi = 0$ at the inlet (feed) where $z = 0$, and runs to $\xi = 1$ at the outlet of the upstream compartment (retentate).

We use the model for removal of neutral solutes in an RO membrane as discussed in previous section, neglect the diffusion boundary layer (DBL), and thus use Eq. (22) for solute flow, and Eq. (35) for water flow, each evaluated at all positions z (or ξ) in the module. Flow along the membrane is by advection only, thus backdiffusion in the z-direction through the module is not considered. An overall balance is used describing that the sum of volume flow rates on the upstream side (high pressure side) and on the downstream side (low pressure side) at that same z-position, is equal to the volume flow rate of the feedwater. A similar overall balance in salt flow rates can also be set up. Combination of these two balances leads to

$$c_p = \frac{c_f \phi_{v,f} - c \phi_v}{\phi_{v,f} - \phi_v} = \frac{c_f - c \cdot f}{1 - f} \tag{36}$$

which relates the solute concentration on the downstream side, i.e., the permeate concentration, c_p, at any z-position, to concentrations and

---

[3] The term retentate, with index 'r', from now on refers to the <u>exit</u> of the upstream side. We use 'p' for the z-position dependent permeate concentration within the module, while the exit on that side is denoted as 'p, exit'.
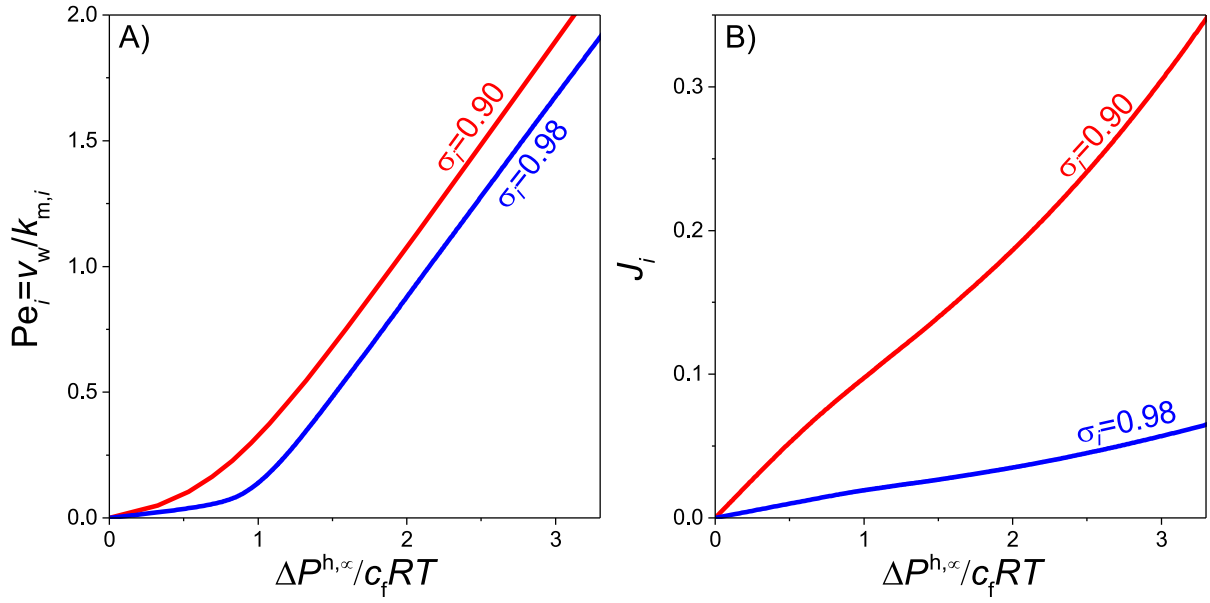
Fig. 4. Permeate water flux v_w (expressed as a Pe-number) and the molar flux, J_i, of a neutral solute as function of $\Delta P^{h,\infty}$, normalized by the feed osmotic pressure, $c_f RT$, across an RO membrane in a 1D geometry. Results of calculations related to Fig. 3 ($k_{dbl,i}/k_{m,i} = 5$, $\beta = 1$).
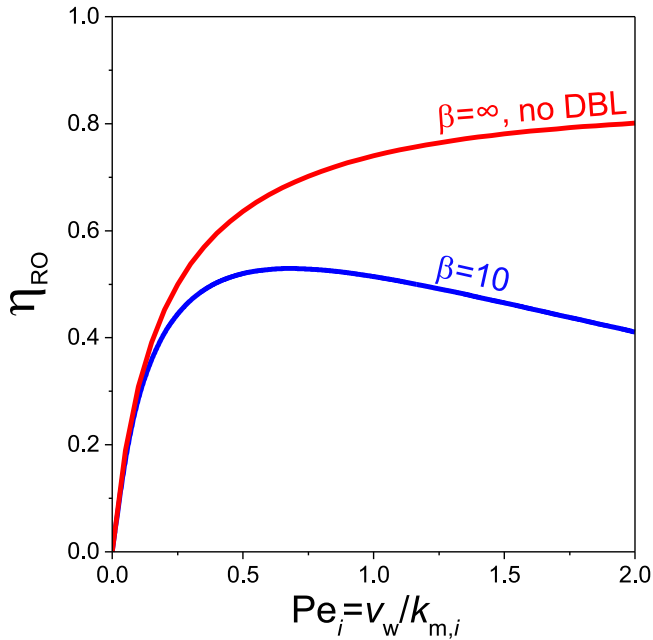

Fig. 5. Energy efficiency, η_{RO}, of an RO membrane process with neutral solutes in a 1D geometry. Results of calculations related to Figs. 3 and 4 ($k_{dbl,i}/k_{m,i} = 5$, $\sigma_i = 0.90$).

flow rates on the upstream side (at the same z-position), and to the feed concentration, c_f. We also introduce here a dimensionless upstream flowrate f, given by $f = \phi_v/\phi_{v,f}$. This factor f starts at $f = 1$ at $\xi = 0$, and decreases with ξ, to reach $f|_{\xi=1} = 1 - WR$ at $\xi = 1$. The z-position-dependent concentration and flowrate on the upstream side are denoted as c and ϕ_v, and have no additional index from now on.

In steady-state, we have on the upstream side a differential balance for the volumetric flow rate given by

$$\frac{\partial \phi_v}{\partial \xi} = -v_w A \tag{37}$$

where A is the total membrane area in the module. A differential balance for the solute flow rate is

$$\frac{\partial (c\,\phi_v)}{\partial \xi} = -J_i A. \tag{38}$$

Both equations can be discretized in various ways and solved, for instance using the backward Euler-method, which is equivalent to modeling N ideally stirred tanks in series [39]. We solve these two differential balances together with flux equations such as Eq. (22) for J_i (with $c_{f,i}$ replaced by c).

Intriguingly, in the limit that $Pe_i \gg 1$, thus when Eq. (24) can be used, then together with Eqs. (37) and (38) we obtain the elegant result that at each position in the module water flowrate and solute concentration on the upstream side are related by

$$\frac{c}{c_f} = \left(\frac{1}{f}\right)^{\sigma_i}. \tag{39}$$

We can apply Eq. (39) to retentate stream, where $f = 1 - WR$, and in this way calculate c_r. With Eq. (36) we can subsequently calculate the exit permeate concentration, $c_{p,exit}$. Indeed, with the development of Eq. (39), we can now quickly evaluate the retention that can be achieved in a module. In the 1D calculation earlier on in this section, in the advection-dominated limit, retention was given by $R_i = \sigma_i$, but in a 2D module, retention is always less, as follows from combining Eqs. (2), (36), and (39), resulting in

$$R_i = 1 - \frac{c_{p,exit}}{c_f} = 1 - \left(1 - (1 - WR)^{1-\sigma_i}\right)\Big/WR \tag{40}$$

which in the limit of low water recovery simplifies to

$$R_i = \sigma_i - \tfrac{1}{2} \cdot \sigma_i \cdot \left(1 - \sigma_i\right) \cdot WR + \cdots \tag{41}$$

which indicates how in the limit of WR $\to 0$ we end up at the result arrived at earlier for the 1D model, that for very low water recovery we have a retention of $R_i = \sigma_i$, but when WR increases this retention drops. So a high water recovery is nice, but will always go at the expense of retention. This is because of the increasing concentration on the upstream side as we move through the module, and thus the solute concentration of the water that flows through the membrane further down the module is higher than earlier on, which reduces module retention.
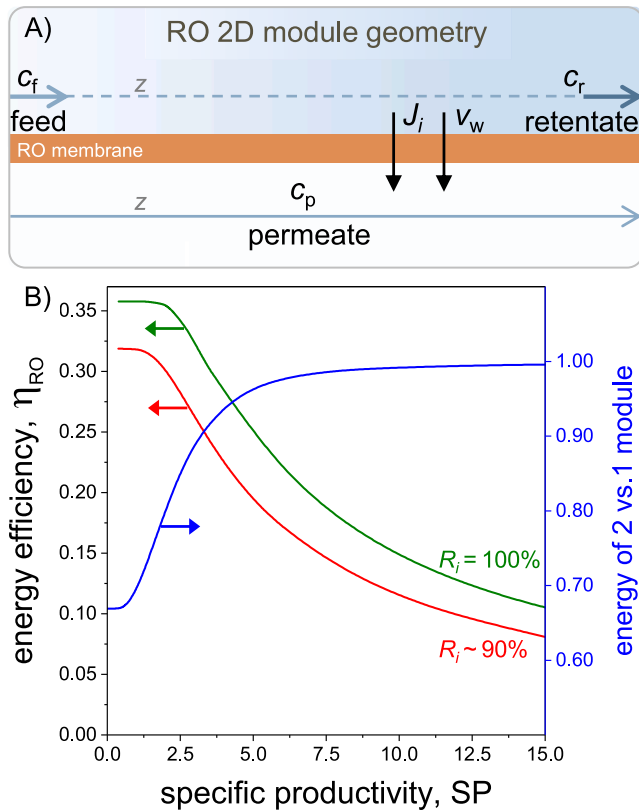
Fig. 6. Theoretical results of 2D RO module calculations with neutral solutes. (A) Schematic diagram of co-current flow 2D RO model. (B) Calculated energy efficiency, η_{RO}, against specific productivity, SP (WR = 80%, $\eta_{ERD} = 50\%$). Red line is for $\sigma_i = 0.95$, in which case retention is $R_i \sim 90\%$. green line is for 100% retention. Blue line describes energy consumption when using two smaller RO modules in series instead of one larger module for $\sigma_i = 0.95$.

The pressure that must be applied follows implicitly from solving a single differential equation for f versus ξ, which is based on combining Eqs. (35)–(37), leading to

$$-\frac{SP}{WR} \cdot \frac{\partial f}{\partial \xi} = \frac{\Delta P^{h,\infty}}{\Pi_f} - \frac{\sigma_i}{1-f}\left(\frac{1}{f^{\sigma_i}} - 1\right) \quad (42)$$

where we introduce the specific productivity SP, a dimensionless parameter given by $SP = \langle v_w \rangle RT / \left(k^{\dagger}_{F-m}\Pi_f\right)$, where $\langle v_w \rangle = WR \cdot \phi_{v,f}/A$ is the permeate water flux, averaged over the module. In the numerical calculation, for any value of SP and σ_i, the pressure ratio $\Delta P^{h,\infty}/\Pi_f$ is varied until solving this equation from $\xi = 0$ to $\xi = 1$ leads to f going from $f = 1$ to $1 - WR$.

Now, we first analyze the minimum pressure and maximum efficiency in an RO module, which can be achieved in the limit of a low permeate water flux, v_w. The pressure required in this limit is what is needed to push the water through the membrane to just reach the required concentration at the exit of the module, c_r, in this limit of low SP. Thus – based on Eq. (35) – the minimum pressure is

$$\Delta P^{h,\infty,min} = \sigma_i \left(c_r - c_{p,exit}\right) RT . \quad (43)$$

This pressure can be multiplied by a factor $\phi_{v,f}\left(1 - \eta_{ERD}\left(1 - WR\right)\right)$ where η_{ERD} is the efficiency of the energy recovery device (to recover energy from the pressure of the retentate flow), to obtain a total energy input. The thermodynamic minimum energy follows from Eq. (12) (without the factor 1/2 because we discuss neutral solutes at the moment), multiplied by the flow rate of all permeate water produced, $\phi_{v,prod}$. The ratio of this thermodynamic energy over the total energy input, is the efficiency η_{RO}. For the calculation we discuss below, with $\eta_{ERD} = 0.50$ and certain values for the setpoints for WR and R_i, we

obtain a maximum efficiency of about 32%, see Fig. 6B. If we assume that the membrane perfectly blocks all solutes ($\sigma_i \to 1$), we can derive for the maximum efficiency

$$\eta_{RO,max} = -\left((1 - WR) \cdot \ln(1 - WR)\right)\big/\left(1 - \eta_{ERD}(1 - WR)\right) . \quad (44)$$

At the same WR as before of 80%, according to Eq. (44) we have a maximum efficiency of ~36%, thus the non-unity value of σ_i in the full calculation leads to a moderate lowering of the RO efficiency. When we operate at lower WR, we can increase efficiency up to a maximum efficiency of 41% when WR = 53% ($\sigma_i = 0.95$). Higher efficiencies are possible with higher η_{ERD} with a further reduced WR (for $\eta_{ERD} = 90\%$, we have 60% efficiency at WR = 32%, again $\sigma_i = 0.95$). Note that these are maximum efficiencies in the limit of low SP.

Full calculations, also for higher SP, are presented in Fig. 6B, which plots energy efficiency η_{RO} versus specific productivity, SP. Starting at a maximum value of η_{RO} at low SP, η_{RO} steadily drops with increasing SP. Cost calculations will determine where on this curve is the optimal point of operation. The curve depends on water recovery and on σ_i, but interestingly, it does not depend on c_f or on the water–membrane friction, $k^{\dagger}_{F-m}$. A higher $k^{\dagger}_{F-m}$ leads to movement along the curve to lower SP, but we stay on the curve. The same for a lower feed concentration, which via $\Pi_f = c_f RT$ has the effect that SP goes up and thus – moving along the curve – η_{RO} goes down. So when we remove solutes at given values of WR and retention R_i (such as WR = 80% and $R_i = 90\%$), energy efficiency decreases when c_f decreases.

3.6. Efficiency and cost analysis for a 2D RO model

Having analyzed energy efficiency, we can make a preliminary cost analysis for optimal operation of an RO module using the RO model discussed in the last section. Optimal RO operation minimizes the sum of two cost factors, first the energy use, and second material costs. The energy costs are the product of five factors: 1. the costs of a unit of energy CUE (in an arbitrary monetary unit, per J of energy); 2. a multiplier m_1 for the total energy use in a unit or plant, over that required to generate the pressure in the RO unit; 3. the factor RT; 4. the feed flow rate $\phi_{v,f}$; and 5. the required energy per m³ feed stream. The material costs are the product of four factors: 1. the costs to purchase membranes, CMP (in the same monetary unit as above, per m²); 2. a multiplier m_2 to relate to other plant expenses, assumed to be proportional to the installed membrane area; 3. the required area A; and 4. one over the lifetime of the membrane, i.e., the operational time Δt that a membrane can sustain before it must be replaced. The energy per m³ feed stream is the applied pressure multiplied by a term that accounts for the recovery of pressure energy, thus $\Delta P^{h,\infty}$ times a factor $1 - \eta_{ERD}(1 - WR)$. We add up energy and material costs to arrive at the total costs (per time of operation)

$$TC = m_1 \cdot CUE \cdot \phi_{v,f} \cdot \Delta P^{h,\infty} \cdot \left(1 - \eta_{ERD}(1 - WR)\right) + m_2 \cdot CMP \cdot A/\Delta t . \quad (45)$$

Because we define efficiency as $\eta_{RO} = E_{min} \cdot WR/\left(\Delta P^{h,\infty} \cdot (1 - \eta_{ERD}(1 - WR))\right)$, Eq. (45) becomes

$$tc = \frac{\alpha \cdot ec_{min}}{\eta_{RO}} + \frac{1}{SP} \quad , \quad \alpha = \frac{m_1 \cdot CUE \cdot k^{\dagger}_{F-m} \cdot \Pi_f^2 \cdot \Delta t}{m_2 \cdot CMP \cdot RT} \quad (46)$$

where $ec_{min} = E_{min}/\Pi_f$, where tc is the dimensionless total costs per unit product, and where the cost factor α is dimensionless as well. This factor is proportional to the cost of energy, and inversely proportional to the cost of purchasing the membranes. Thus less expensive membranes increase this factor α.

We make a calculation based on the $(\eta_{RO} - SP)$–curve of the last section for $\sigma_i = 0.95$, and obtain the result that for $\alpha = 0.01$ we have an optimum SP = 8.34, and when α increases tenfold (energy 10× more expensive, or membranes 10× less expensive), then SP drops to 2.95, i.e., the optimum situation is now at an almost 3× larger system (for the same production of water). If the change in α is because of an increase in energy costs, then after the optimization, the total operational costs
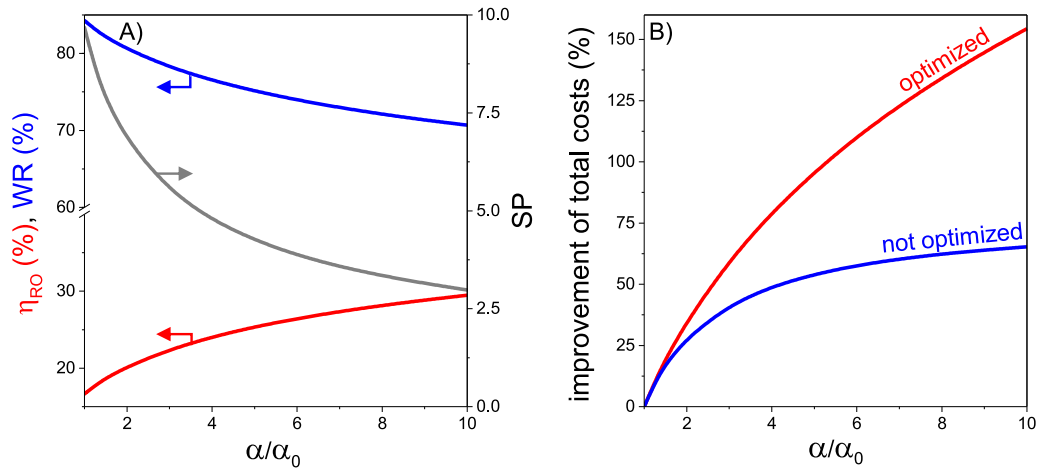
Fig. 7. Results of cost optimization of RO module for perfect retention, $R_i = \sigma_i = 1$, as function of an increase in the cost factor α/α_0 (a factor describing energy over material costs) leading at each α to a different optimum for WR and SP, and a different η_{RO}. Panel B is based on α increasing because material costs go down, with energy costs unchanged. In this case, less expensive membranes lead to a higher energy efficiency, η_{RO}.

is only a factor of 4 larger, not 10. And when the increase in α is because membrane purchase costs decreased by a factor of 10, then without further system modifications this would lead to a reduction in the total costs by a factor of 1.7, but after optimization (installing more membranes, thus reducing SP) a cost reduction by a factor 4 is achieved.

Thus this calculation shows that when energy costs increase, thus α increases, that the system should be operated at higher efficiency and lower SP, i.e., it becomes favorable that more membranes are purchased and installed. And the same result is obtained for the case that the purchase costs of membranes goes down (or we make improvements such that we can use them longer, i.e., Δt goes up), then α also goes up, and we also want to run the desalination plant at lower SP and higher efficiency η_{RO}. Thus, because of cost optimization, 'less expensive membranes have higher efficiency'. This conclusion, here arrived at for neutral solutes, likely also applies for RO with salt solutions. In the next section we make a similar analysis for ED.

In a second calculation we investigate the influence of water recovery. When the aim is to make an optimization for the same retention, we face the issue that retention depends on water recovery. This can be dealt with by including a bypass of feedwater to the product stream (if the realized retention is higher than the setpoint for retention), or by assigning a pecuniary penalty to any offset in retention. Because we do not want to deal with these complications now, we assume in what follows that retention is perfect, i.e., we set $\sigma_i = 1$. Then retention is always the same, namely 100%.

In that case the differential equation (42) leads to the analytical result

$$\text{WR} \cdot \gamma - \ln\left(1 - \text{WR} \cdot \gamma / (\gamma - 1)\right) = \text{WR} \cdot \gamma^2 / \text{SP} \quad , \qquad \gamma = \Delta P^{h,\infty} / \Pi_f \quad (47)$$

and together with Eqs. (13) and (46), we can make the calculations presented in Fig. 7 where for each value of α we can now find the optimum WR and SP. With an energy recovery device with an efficiency $\eta_{ERD} = 50\%$ and an initial cost factor $\alpha = 0.01$, then the system has the following optimized properties: WR $\sim$ 84.3%, $\eta_{RO} \sim$ 16.6%, and SP $\sim$ 9.68. As Fig. 7A shows, when the factor α goes up, either because material costs are lowered or the price of energy goes up, the new optimum is at a higher energy efficiency η_{RO}, with SP going down because we push the water through at a lower rate per unit membrane area, with a significantly increased size of our module: in Fig. 7A, we can see that SP goes down from $\sim$9 to $\sim$3 when α is increased by a factor 10, which then implies that it becomes favorable to increase the total area in the membrane modules by a factor of $\sim$3 (for the same amount of water that is treated). The optimal water recovery decreased from around 84% to 71% when α increases by a factor of 10.

We now assume that the increase in α is because we are able to reduce the material costs, either by extending the lifetime of membranes or by reducing CMP, both of which will increase the cost factor α. We then arrive at a percentage-wise improvement (reduction) in total costs as depicted in Fig. 7B, first simply by factoring in that material costs go down, without redoing the optimization, and secondly after a renewed optimization which further improves the cost reduction. The corresponding new values of η_{RO}, WR, and SP, are depicted in Fig. 7A. The end result is that the energy efficiency of the process goes up significantly, and this happens in some sense 'because' the materials were less expensive.

Of course this analysis was only an example calculation, and a large range of factors is neglected, such as the effect of the DBL on transport, the dependence of fouling on transmembrane flowrates, and many other process constraints. And again, this entire calculation was for a membrane that under all conditions perfectly blocks the solutes, which is not the case in reality. And the calculation was for a neutral solute, not for a salt solution... Another assumption was that the hydrostatic pressure on the upstream side was set to a constant factor, neglecting the decrease in pressure between inlet and outlet (order of 0.2 bar) [40]. Another cost factor that is relevant to include is that of water pretreatment. Pretreatment costs scale linearly with feed flow rate, so is inversely proportional to water recovery (for a given system permeate production). Yet another factor is brine disposal which has an associated cost [40], and if that is proportional to the volume thereof (and not on the total amount of salt in there), then another factor must be included that scales with $(1-\text{WR})/\text{WR}$, which would shift the optimum to a higher WR. Optimization studies that incorporate these effects are very useful. Also of interest are calculations that incorporate that in RO the direction of flow of permeate is at right angles to the flow direction on the retentate side, i.e., in the module flow is in crosscurrent mode. For ED we discuss crosscurrent flow in Sections 6.3–6.5.

3.7. Optimization for two combined RO modules in a system

Let us next analyze what advantage can be achieved when we work with two RO modules, not one, as also analyzed in Ref. [41]. When we compare with a single module, the ratio of total water throughput over total membrane area must be the same, i.e., with two modules, on average they must be twice as small. In the calculation we make, the retentate of module 1 is directed to module 2 that operates at a higher pressure. The same overall setpoint applies as in Section 3.5 of 80% water recovery. We again use $\sigma_i = 0.95$ and $\eta_{ERD} = 50\%$.

What we find is that there is a positive effect of the use of multiple units when we work at low SP, in the region where efficiency is at

a maximum, see Fig. 6 [1]. Now, in that limit, with two modules in series, efficiency η_{RO} can increase significantly, from ~32% to ~48%. At the optimum, water recovery is almost the same in both units, at a value of ~55%, similar to statements in Ref. [41] and references in there. Furthermore, we find that the pressure in the second unit is about 2.2× that of the first module. (Thus the retentate of module 1, which is about 45% in volume of the feed stream, is further increased in pressure by 1.2× what was the pressure applied to the water entering the first module.) However, with increasing SP the advantage decreases, the optimal ratio of pressures decreases from the factor 2.2 to 1.0, i.e., the two pressures in the modules become the same. Or in other words, there is no advantage any more of using two modules. This observation, that using multiple modules is not always better, may go against a common notion on the design of RO systems where the general idea is that more units are always better, because then we do not have to push so hard in the first module where solute concentrations are still low. However, our calculations show this is only the case at low SP.

This finalizes the discussion of various aspects of the modeling of an RO unit to remove neutral solutes. In Section 6 we discuss 1D and 2D calculations of an RO module with a symmetric 1:1 salt solution.

4. A simple model for electrodialysis for symmetrical cell pairs

A simple model for electrodialysis can be derived by an approach that we will outline next. In electrodialysis feedwater flows into two adjacent sets of channels, see Fig. 1B. In one series of channels the water will be desalinated, which are the diluate channels, denoted by 'd'. Salt ions move from these d-channels to the concentrate 'c' channels. In many practical ED stacks, the flow pattern in each channel is in first approximation 'at 90 degrees' to the flow pattern in adjacent channels. This is called a cross-flow geometry. This geometry is more complicated to model, and thus in this section we assume that we have perfect co-current flow, i.e., we assume a one-dimensional geometry where the two flows enter the module from the same side and flow in the same way on either side of the membranes. The two channels can still be different in width and the flowrates (thus residence times) can be different.

An ED stack has two electrodes on either end where electronic current is transferred to ionic current. In this review we do not discuss the electrodes but we focus on the repeating unit of an ED stack, which is the membrane cell pair, see Fig. 1B, which consists of two membranes and two flow channels. As mentioned, in the flow channels we assume co-current flow of the water along the membranes, from inlet to exit of the channel. While the water flows through these thin channels between the membranes, ions move from the d-channels to the c-channels by transport across the membranes. This process is possible because – driven by the electrical current – anions move in one way out of each d-channel, to be transported through membranes that are selective for anions. These are 'anion-exchange membranes' or AEMs, which are membranes in which the water-filled pores are lined with high concentrations of positive membrane charges (of the order of 5 M fixed membrane charge per volume of water in the membrane). The cations move in the other direction, passing cation-exchange membranes, or CEMs. These CEMs have a high concentration of fixed negative charge, again of the order of 5 M, and they preferentially allow access to cations, largely blocking the passage of anions. Each d-channel has such an AEM on one side, and a CEM on the other. The net effect of this layout of a cell pair, of a sequence of an AEM, d-channel, CEM, and c-channel, and this repeated tens to hundreds of times, is that the d-channels are being desalinated, while the salinity in the c-channels increases between entrance and exit of each channel. Thus in the AEMs anions are the main charge carrier, while in the CEMs cations carry most of the charge. These ions in their respective membrane are the counterions (anions in an AEM, cations in a CEM). The minority ions, that ideally are fully blocked, are called coions (cations in AEM, anions in CEM).

<u>Explanation of coion leakage in ED.</u> Let us describe the functioning of the ED cell pair in an alternative manner. With the current directed to the right, cations will flow rightward, and anions will flow leftward. In the bulk of the channels, for a symmetric system, this current is equally carried by cations, moving right, and anions that move left. Cations and anions can have velocities in this left–right direction that tend to zero (near a blocking membrane), but they do not flow 'back' at any point in the module. With AEMs and CEMs alternatingly placed in the stack, and with cations moving right, anions left, then the following will happen. One type of channel has a CEM on its right side. That membrane freely allows the cations to pass to the next channel (to the right). And that same channel has an AEM on its left side, and anions can pass that membrane freely and move left. But now, in these adjacent channels, things are different. The anions want to continue moving left, but now they encounter a CEM which blocks them. And cations that want to move right, encounter an AEM that blocks them. So in this second set of channels, the ions accumulate, and thus the salt concentration increases. These channels will be the concentrate channels. Ions that arrive in these channels, cannot escape.

What was just described, is the ideal functioning of an ED stack, and it is generally like this early on in a cell pair, where current densities are still high and concentration differences between the two types of channels, c_d and c_c, still low[1]. But further on in the stack, with $c_c \gg c_d$, ions start to leak from the concentrate channel. They leak in the direction that drives them onward, not back to the diluate channel that they came from, but on to the *next* diluate channel. The membrane that blocked them from leaving the concentrate channel in the ideal case (e.g., the AEM for a cation), becomes leaky. Why is that? Chemically the membrane is of course the same as before. But this increased coion leakage from the concentrate channels is because the increasing concentration difference across this membrane leads to more and more diffusion of coions. Indeed, diffusion is the main membrane transport mechanism for co-ions in ED. Thus further on in a cell pair, the driving force for diffusion increases, and thus ions that were kept in the concentrate channel quite well at first, now increasingly leak out; so cations that entered a concentrate channel on the left side, now leak out on the right side.

It now turns out to be the case that this leakage is more pronounced for membranes that have a high diffusion coefficient, and for membranes that are thin. With thin membranes, the gradient in concentration across the membrane is steep, and we therefore have a large driving force for diffusion [42]. To avoid this leakage from the concentrate channel, membranes should not be too thin (a thickness of at least 10 μm is a well-known estimate). This increased leakage is a reason why, towards the exit of a channel, the net rate of salt removal goes down (per unit membrane area). The other reason is that the local current density goes down, so the transport of ions from diluate to concentrate channels (the intended purpose of ED) also goes down. This decrease is because the resistance goes up in the diluate channel, and Donnan potentials increase. So for a given cell pair voltage, V_{cp}, the high current densities that could be achieved early on in the channel, are dropping significantly the further one progresses down the channels. Thus the flux of cations and anions arriving in the concentrate channels goes down significantly. And at the same time diffusional leakage goes up, as discussed. As a consequence, at some point in the channel a condition is reached that current is still running, but the net salt transport from diluate to concentrate channels (arrival minus leakage) drops to zero. At this point (and beyond), the *current efficiency*, λ, reaches the value of zero. This limiting value of $\lambda = 0$ will be used further on to calculate the 'final' current density and salt concentrations, c_d and c_c, in a stack run at a fixed cell pair voltage.

[1] The same analysis applies to a (short, or 'differential') stack that is fed from reservoirs to which the effluent also flows back (batch-mode ED operation, solution is recirculated between the reservoirs and the stack, and is desalinated over time). Then statements about 'early on in the stack' can be changed to 'early in time', and 'further on' by 'later', assuming we started with two reservoirs at equal salt concentration. Note that in this layout, the stack can be run at constant voltage or constant current. Instead, in the calculation of co-current flow in a single stack without these reservoirs, then in the common design with two undivided end-electrodes, then the entire stack is operated at one value of the cell pair voltage, and the further we are away from the entrance, the lower is the current density.

In a later section we discuss how to optimize ED operation by having multiple ED stacks in series with different water velocities and operational currents, but for now we discuss a single cell pair. In the simple model we discuss, we neglect water transport through the membranes. Unfortunately, in reality this water flow is not zero, and has a tendency to lower ED performance, but for now we neglect it. Thus the water recovery, WR, is directly set by how much of the feedwater flows to the c-channels and how much to the d-channels, namely $WR = 1/\left(1 + \phi_{v,c}/\phi_{v,d}\right)$. Thus, for equal flow rates to the two channels, we have $WR = 0.50$.

We set up for each channel a steady-state plug flow model, with ion transport through the membranes in a 'sideways' direction. In each channel, at each position z, where z is the direction along the membranes, there are concentration profiles across the channel, from membrane to membrane, but they can be relatively minor when the channels are narrow.[4] Thus for the moment in each channel we use a z-dependent mass balance that does not have any dependence on position in the perpendicular x-direction, which is the direction towards the membranes, at right angles to the z-direction of water flow along the membranes. Then a mass balance for an ion i at some position in a flow channel becomes

$$p \frac{\partial c_i}{\partial t} = -v_z \frac{\partial c_i}{\partial z} \pm a \cdot \left(J_{\text{AEM},i} + J_{\text{CEM},i} \right) \tag{48}$$

where p is the porosity (open volume fraction) of the channel, v_z the velocity of the water through the channel, in the direction along the membrane. This is an average velocity, i.e., it is a water flowrate in m^3/s divided by the cross-sectional area of a channel (the cross-section through which the water flows). It is a superficial velocity, i.e., the presence of a spacer material that reduces p does not change the numerical value of v_z. The specific membrane surface area is a, which is the area of one membrane lining a channel divided by the channel volume. And thus $a = 1/L_{\text{ch}}$, where L_{ch} is the width of the channel. We use the symbol $\pm$ in Eq. (48) to avoid technicalities of how to define the directions of fluxes, because that is not essential at this moment.

We now consider a binary 1:1 salt. We add up Eq. (48) for anions and cations, assume steady-state, thus the term $\partial c_i/\partial t$ is zero, and consider that at each position z we have electroneutrality, i.e., $c_+ = c_-$, and from now onward we use c_j for the salt concentration, i.e., $c_j = c_{+,j} = c_{-,j}$ which is z-dependent, and different between the c- and the d-channels (the two channels are referred to by index j). Thus we add up Eq. (48) for the two ions, and then divide by 2. The summation of the four fluxes $J_{i,\text{IEM}}$ is twice the total salt flux, J_{salt}, which is the flux of salt from d- to c-channels, per unit area of one membrane, as a summation of the two membranes together. We then arrive at

$$v_z \frac{\partial c_j}{\partial z} = \pm a_j J_{\text{salt}} = \pm a_j \lambda_{\text{cp}} \frac{I}{F} \tag{49}$$

where we introduce the current efficiency λ_{cp}, a process parameter that is z-dependent in the cell pair, i.e., $\lambda_{\text{cp}}(z)$, and we introduce the current density I in A/m^2. In an ED stack, in a cell pair, from entrance to exit (i.e., from $z = 0$ to $z = \ell$, with ℓ the length of the channel in flow direction), current density I will change with z. We cannot make the current constant in a normal ED stack. This is because there are two end-electrodes that have a certain voltage between them. Therefore it is the cell pair voltage, V_{cp}, which will be the same at each z-position in the cell, and because Donnan potentials and resistances increase with z, current will decrease in that direction.

Eq. (49) introduces a cell-pair based current efficiency λ_{cp} which relates to the total salt transport flux between the d- and c-channels, J_{salt}, and the current, I, all z-dependent. To calculate λ_{cp} and J_{salt} we

must solve at each z-coordinate a membrane model for the AEM and the CEM, and in each membrane describe the flow of counterions and coions. In such a model all parameters, including the diffusion coefficients of the ions, and the membrane charge, can be different between AEM and CEM. This calculation is possible, but in this review we simplify this situation, and assume the AEM and CEM are each other's perfect 'mirror image'. Thus, the fixed membrane density in an AEM, denoted by the symbol X, has the same magnitude as the membrane charge of a CEM, and only the sign of these two charges is opposite to one another. Furthermore, the diffusion coefficient of the counterions in the AEM and CEM is the same, and the same for the coions (coions and counterions can still have diffusion coefficients that are different from one another). With these assumptions, the cell-pair based λ_{cp} is now the same as a 'single membrane'-based current efficiency λ_{th}, where we use the subscript 'th' for 'theoretical' because this single membrane-efficiency cannot be measured but can be obtained from a theoretical model of a single ion-exchange membrane (IEM), as we will do in this section.

Thus, in each of the two channels of an ED cell pair, we now have the mass balance

$$v_{z,j} \frac{\partial c_j}{\partial z} = \pm a_j \lambda_{\text{th}} \frac{I}{F} . \tag{50}$$

Eq. (50) can be solved as function of z if we know $I(z)$ and $\lambda_{\text{th}}(z)$, and to do that, at each position z two algebraic equations (AEs) must be solved jointly with Eq. (50) in each channel. Because the right side of Eq. (50) is the same for each channel, except for the $\pm$ sign, and except for a_j, we can add up these two balances over the two channels, and arrive at

$$L_{\text{ch}} v_z \frac{\partial c}{\partial z} \bigg|_{\text{d-channel}} + L_{\text{ch}} v_z \frac{\partial c}{\partial z} \bigg|_{\text{c-channel}} = 0 \tag{51}$$

where we implemented how in each channel $a_j = 1/L_{\text{ch},j}$. Eq. (51) can be integrated from the inlet to a certain position z. When we have an equal inlet concentration $c|_{z=0}$, namely equal to the feedwater concentration, c_f, we arrive at

$$\phi_{v,d} \left(c_d(z) - c_f \right) + \phi_{v,c} \left(c_c(z) - c_f \right) = 0 \tag{52}$$

where we converted from flow velocities v_z to flow rates in each channel, $\phi_{v,j}$, by multiplying each side by the geometrical 'depth', which is the membrane area divided by the path length ℓ. Thus we end up with an equation describing how all salt that is removed from one channel ends up in the other channel. Eq. (52) is an AE that becomes part of the model and it replaces the ODE for one of the channels. Thus, the full ED model (co-current, steady-state, symmetry, ...) consists solely of one ODE and three AEs, to be 'tracked' along a coordinate z from entrance to exit of the cell pair. Note that still WR can have any value, and also the width of each channel can be different, thus the residence time in the d- and c-channels can be very different.

Now, interestingly, for any c_d we see from Eq. (52) that c_c automatically follows, and as we show below, for a given cell pair voltage, V_{cp}, then λ_{th} and I also follow automatically. Thus, there is no particular dependence on position z. Thus, we can also rewrite the one remaining ODE, that we will evaluate for the d-channel, and we take I as a positive number, to

$$\frac{\partial c_d}{\partial t^*} = -a_d \lambda_{\text{th}} \frac{I}{F} \tag{53}$$

where the time-on-stream, t^*, is given by $t^* = z/v_z$. This representation shows that this model is equally valid for two very different cases: first, the above-discussed geometry of an ED cell pair with two co-current flow channels, and second the same model also applies for an ED stack with relatively low desalination 'per pass' where the effluents of each channel are rerouted to two storage tanks from which the same channel is fed again. Now t^* really is a time. In that case, the area/volume ratio, a_d, in Eq. (53) is changed to the area of one membrane times the number of cell pairs, divided by the volume of the d-reservoir

---

[4] This is not always the case, and sometimes these profiles do matter significantly. Also with three or more different ions, instead of a simple binary salt, the situation in the flow channels can become radically different, and concentration profiles across the channel must then be considered.

(including volumes of tubing and the channels in the ED stack). The final modification is that in Eq. (52), we replace volume flow rates by the two reservoir volumes. Note that the model as presented assumes no volume flow through the membranes, but this effect can be included with few modifications. Let us point out again that despite the appearance of a 'time' t^*, nevertheless at the level of the membrane this is a steady-state process model.

To solve this model, we can calculate the time step Δt^* when we let c_d step downward in fixed increments starting at an initial value. We can use the Crank–Nicolson scheme in which λ_{th} and I are averaged between known values at subsequent 'c_d-lines', at k-1 and k, according to [39]

$$\frac{c_{d,k} - c_{d,k-1}}{t_k^* - t_{k-1}^*} = -\frac{a_d}{F} \cdot \frac{1}{2} \cdot \left(\lambda_{th,k-1} I_{k-1} + \lambda_{th,k} I_k \right). \tag{54}$$

Now we only have to formulate expressions for current efficiency, λ_{th}, and for current density, I, as function of c_d and cell pair voltage V_{cp}. This is discussed in the next section.

4.1. Calculation of current and current efficiency in ED

To calculate current and current efficiency, we must first relate current density I to the voltage drops over the membranes and flow channels. The cell pair voltage, V_{cp}, is a summation of the voltage drops across two channels (d- and c-channels), two membranes (AEM and CEM), and in total four Donnan potential drops (at each channel/membrane interface in the cell pair). For a symmetric system, the four Donnan potentials simplify to two times the same difference between two Donnan potentials. In the symmetric model we also assume each membrane has the same resistance. The two channels will, as desalination progresses, have very different resistances. In each membrane, the relationship between current and voltage can be described by

$$I = \pm k_m |X| F \Delta\phi_m \tag{55}$$

where k_m is a membrane transport coefficient, $|X|$ is the magnitude of the membrane charge density, and $\Delta\phi_m$ is a dimensionless potential, or voltage, drop across the membrane. This voltage drop is only across the inner part of the membrane, excluding the voltage changes (Donnan potentials) at the two edges of each membrane. These we will discuss further on. Eq. (55) assumes that both ions have the same diffusion coefficient in the membrane, D_m, and thus the mass transfer coefficient k_m, which is the ratio of this D_m over membrane thickness, L_m, is the same for both ions. This diffusion coefficient will be much lower than in free solution, because of membrane porosity, tortuosity, and the small pore size. For instance, diffusion in the membrane will be slower by a factor of 20–50 compared to outside, in free solution. Eq. (55) furthermore assumes that the membrane charge density, $|X|$, is large compared to salt concentrations outside the membrane. (In a generalized version of Eq. (55), the term $|X|$ is replaced by an average total ions concentration, $\langle c_{T,m} \rangle$.) Any voltage ϕ can always be multiplied by the thermal voltage, $V_T = RT/F \sim 25.6$ mV (at room temperature), to arrive at a dimensional voltage in (m)V.

Similar to Eq. (55), we have a current–voltage relationship across the d- and c-channels, given by

$$I = \pm 2 k_{ch,j} c_j F \Delta\phi_{ch,j} \tag{56}$$

where $k_{ch,j}$ is a channel transfer coefficient, given by $k_{ch,j} = \varepsilon D_\infty / L_{ch,j}$, where D_∞ is the diffusion coefficient of ions in free solution. The factor ε is the channel porosity p divided by a tortuosity factor τ, i.e., $\varepsilon = p/\tau$, and describes how in the spacer channel the effective diffusion coefficient for electromigration is lower than in free solution, because of a spacer structure that fills the channel. The channel width is $L_{ch,j}$. Note the factor 2 in Eq. (56) which relates to both anions and cations contributing equally to current flow. Eq. (56) is valid when the

two ions have the same diffusion coefficient,[5] and in the absence of concentration gradients across the channel.

Next we consider the four Donnan potential drops at the four membrane/solution interfaces. In the symmetric system we discuss, the two Donnan drops at the AEM are exact mirror-images of those at the CEM because we assume the same $|X|$ for AEM and CEM, so we only have to discuss one of these membranes here. We continue to assume that we only have monovalent ions in solution. We neglect all ion partitioning effects other than the Boltzmann distribution that relates to the charge of ions. This Boltzmann equation for each ion, distributing between just in the membrane and just outside, is

$$c_{m,i} = c_{\infty,i} \exp\left(-z_i \Delta\phi_D\right) \tag{57}$$

where ∞ refers to a position just outside the membrane (in the ED model z-dependent), and Eq. (57) applies to the interface of the membrane with electrolyte in the d- and c-channels. The Donnan potential at each of these interfaces is the potential just in the membrane, relative to just outside, in solution.

Based on electroneutrality in the membrane, valid at each position in the membrane, we have

$$c_{m,+} - c_{m,-} + \omega |X| = 0 \tag{58}$$

where ω is the sign of the membrane charge ($\omega = +1$ for an AEM and $\omega = -1$ for a CEM). Based on Eqs. (57) and (58) we can derive for the Donnan potential that

$$\Delta\phi_D = \sinh^{-1} \frac{\omega |X|}{2 c_\infty} \tag{59}$$

where the function $\sinh(x)$ is identical to $1/2 (\exp(x) - \exp(-x))$, and $\sinh^{-1}$ is the inverse of that function (also written as asinh or arcsinh). Eq. (59) is valid for a solution with monovalent ions only, and without considering partitioning coefficients other than pure 'Boltzmann' electrostatics. For a detailed discussion on the various contributions to the partitioning coefficient at an interface between free solution and a microporous charged material, see Refs. [17,39]. As Eq. (59) shows, for a membrane with negative fixed charge, i.e., a CEM, which needs to 'pull in the cations', the Donnan potential is negative, i.e., from just outside to just inside the membrane, the potential goes down.

The eight voltage drops described in the above equations can all be added up (taking care of appropriate choices of $\pm$-signs), to arrive after multiplication with V_T, at the cell pair voltage, V_{cp}. And this V_{cp} is invariant with z; see Fig. 2 in Ref. [42] for an example of a voltage profile. (Thus the eight individual voltages described above, they all change with z, but their summation, which is V_{cp}, does not.)

Before we show the result of such a combined expression for V_{cp} versus current, I, and versus channel salt concentrations, c_d and c_c, we first evaluate the Donnan potential, Eq. (59), in a novel, useful, manner. The Donnan potential, as described by Eq. (59), must be evaluated on two sides of the same membrane (and then for two membranes), and because both count 'inside minus outside', the result for a given membrane is

$$\Delta\phi_{D,tot} = \sinh^{-1} \frac{|X|}{2 c_d} - \sinh^{-1} \frac{|X|}{2 c_c} \tag{60}$$

which we can call the total Donnan potential across a membrane. (This excludes the membrane potential across the inner part of the membrane due to current, as given by Eq. (55).) We drop here and below the subscript ∞ when we refer to salt concentrations just outside the membrane. We next evaluate the equation for $\omega = -1$, i.e., a CEM, but for an AEM the same result is obtained with a final overall minus-sign difference. Now, generally, Eq. (60) is not used in this way,

---

[5] As long as we have a binary salt, also for ions of different valency and diffusion coefficient, an expression such as Eq. (56) can always be arrived at, but the harmonic mean diffusion coefficient must be used.

perhaps because it looks somewhat too unwieldy. Instead, in literature the following equation can often be found, which is

$$\Delta\phi_{D,tot} = \pm \ln \frac{c_c}{c_d} \tag{61}$$

and this expression is valid for an ideal membrane, one that perfectly blocks coions. There is no dependence on membrane charge here. A prefactor in front of the ln-term can be added, which is then called permselectivity, which describes the difference between the ideal ln-term and the measured Donnan potential. The $\pm$-symbol depends on the sign of the membrane charge and on whether 'Δ' is defined from c-side to d-side or vice-versa.

Now, interestingly, Eq. (61) follows from Eq. (60) as a first term in a Taylor-expansion around the point that $X^{-1} \to 0$. This first term is very accurate when on both sides of the membrane the salt concentration is very low compared to X. But we can now add the second term in the Taylor expansion and obtain a novel, highly accurate, expression for the Donnan potential, given by

$$\pm\Delta\phi_{D,tot} = \ln \frac{c_c}{c_d} - \left(c_c^2 - c_d^2\right)/X^2 \tag{62}$$

where the total Donnan potential decreases (in magnitude) when membrane charge density X drops, or when the difference between c_c and c_d increases. Note that this novel equation is only valid as a first correction to Eq. (61) when X is of the order of the salt concentration or larger. For lower X, we must use Eq. (60). Note that in Eqs. (60) and (62) it is important to use the same unit for c and for X, either both in M or both in mM, i.e., mol/m^3.

Thus, the new expression provides a correction to the Donnan potential for finite values of X, without invoking the empirical concept of a permselectivity. The additional term correctly identifies that the correction to ideality depends on the membrane charge density X, but also on c_d and c_c, and this clearly highlights how the concept of a permselectivity is not an intrinsic membrane property, but for a given membrane varies with salt concentration, even along the z-coordinate within the same ED module (or changes in time in a batch experiment with changing reservoir concentrations).

In general, for arbitrary salt mixtures, and with other partitioning effects besides pure electrostatics, it is advisable to return to a Boltzmann equation for each ion, Eq. (57), in combination with electroneutrality in the membrane. In further model extensions, we can include how the membrane charge is a function of pH or of the concentration of other ions, such as the Ca^{2+}-concentration just in the membrane (in case these ions adsorb), and these ion concentrations in turn depend on the Donnan potential, thus on X. Also other acid–base associations between ions can be included, such as the protonation of an ion, to go from a basic to acidic state, such as NH$_3$ associating with an H$^+$-ion to NH$_4^+$, of which the distribution depends on pK and local pH [43]. Furthermore, mass transport effects across the channels (especially for solutions with three or more types of ions) will lead to ion concentrations just outside the membrane (which are the concentrations that are used in the Donnan equilibria) that are different from the channel-averaged concentrations at that z-position. Also transmembrane water flow can be of importance, because it 'pushes' ions away from the membrane surface, or pulls them in, and thus also modifies ion concentrations just next to the membrane. All in all, in detailed modeling of an ED cell, the above simplified equations must always be critically evaluated to ascertain whether they are sufficiently accurate for the situation under study.

Now we can finally add up all eight voltages to obtain one final equation. The result shown next assumes that c- and d-channels have the same width, L_{ch}, and we already discussed the assumption that each membrane has the same charge X and the same transport properties, thus the same k_m. We then arrive at

$$\frac{V_{cp}}{V_T} - 2\left(\ln \frac{c_c}{c_d} - \frac{c_c^2 - c_d^2}{X^2}\right) = \frac{I}{F}\left(\frac{1}{2\,k_{ch}}\left(\frac{1}{c_d} + \frac{1}{c_c}\right) + \frac{2}{k_m|X|}\right) \tag{63}$$

where c_c, c_d and current density I are all z-dependent. The placements of the factors '2' at the end of this equation may seem counterintuitive, with one in the numerator, one in the denominator, but they are correct. We can use Eq. (63) to derive the current at the inlet of the stack (or, cell pair), because then both c_c and c_d are equal to c_f, and thus all Donnan effects disappear, and we obtain

$$V_{cp} = \frac{RT}{F^2}\left(\frac{1}{k_{ch}c_f} + \frac{2}{k_m|X|}\right)I \tag{64}$$

which includes two (actually four) resistances in series at each z-position in an ED stack, namely the resistance in each channel and in each membrane. Each resistance is the inverse of a conductivity, and these are respectively $2k_{ch}c_f$ and $k_m|X|$ (both with units mol/m^2/s).

Finally we evaluate the current efficiency λ_{th}, at each z-position. To that end we must establish what is the flux of counterions through each membrane, which is the desired effect, leading to desalination, and the flux of coions, which is a deleterious effect, reducing desalination, because coions leak out of the c-channels to the d-channels. Based on fluxes through a single membrane, we define λ_{th} as

$$\lambda_{th} = F\frac{J_{m,ions}}{I} = \frac{J_{m,+} + J_{m,-}}{J_{m,+} - J_{m,-}} \tag{65}$$

where $J_{m,ions}$ is the total ions flow through a membrane, $J_{m,ions} = J_{m,+} + J_{m,-}$, and the current density is $I = F\left(J_{m,+} - J_{m,-}\right)$. The factor λ_{th} is only defined for desalination of a 1:1 salt, and will always be between 0 and 1, with $\lambda_{th} = 1$ for ideal operation, with only counterion transport through each membrane. In the limit of $\lambda_{th} = 1$, for each unit of charge a full salt molecule is removed from a diluate channel, while in the limit of $\lambda_{th} = 0$ current is passing the membrane, but there is no net salt removal. This last situation develops near the exit of an ED cell where all ions arriving in a concentrate channel leak out again to a next diluate channel, see a box in Section 4. Next, we analyze ion transport, both of counterions and coions, across a membrane. To that end we use the Nernst–Planck (NP) equation that can be solved at any position in the membrane together with local electroneutrality. For each ion, the NP-equation is

$$J_i = -D_{m,i}\left(\frac{\partial c_{m,i}}{\partial x} + z_i c_{m,i}\frac{\partial\phi}{\partial x}\right) \tag{66}$$

where ϕ is the inner-membrane potential, and x is a coordinate directed across the membrane (across the shortest distance, i.e., across the thickness). We neglect advection in the membrane (water flow and the drag thereof on ions). We assume the same diffusion coefficient for anions and cations in the membrane, and thus we can subtract anion flux from cation flux, to arrive at

$$I/F = J_+ - J_- = -D_m c_{T,m}\frac{\partial\phi}{\partial x} \tag{67}$$

where $c_{T,m}$ is the total concentration of the two ions together in the membrane, i.e., $c_{T,m} = c_{m,+} + c_{m,-}$. Let us reiterate again, that all equations in this section only apply to a 1:1 salt with only one type of cation and one type of anion. Even adding one other type of cation of the same charge but with a different diffusion coefficient can significantly change the model outcome, let alone when this ion has a different valency.

Note that current density I in Eq. (67), calculated based on ion transport in a membrane, *is the same* current density that also crosses (at that same z-position) each of the flow channels, and crosses the other membrane too; i.e., there is (at each z-position) only one value of current I, the same at each location across each of the channels, and it has the same value in all the other cell pairs (at that z-position), which are all exact copies of one another. Related to this statement is that this model assumes that all current 'lines' cross the stack at right angles to the channels and membranes, i.e., the current crosses these layers in the shortest direction. This is a highly accurate assumption.

The NP equation for anions and cations also leads to an expression for the total ions flux

$$J_{m,ions} = J_+ + J_- = -D_m\left(\frac{\partial c_{T,m}}{\partial x} - X\frac{\partial\phi}{\partial x}\right). \tag{68}$$

In the derivation of Eqs. (67) and (68), the electroneutrality condition in the membrane is implemented. Note that Eq. (68) makes use of X without a $|\cdots|$-statement, and indeed X here can be negative and positive. Because of steady-state both equations can be integrated across the membrane, leading to

$$I = \pm k_{\mathrm{m}} F \left\langle c_{\mathrm{T,m}} \right\rangle \Delta\phi_{\mathrm{m}} \qquad (69)$$

where the term $\left\langle c_{\mathrm{T,m}} \right\rangle$ is based on an appropriate average of $c_{\mathrm{T,m}}$ between the two sides of the membrane (from just in the membrane very near the diluate channel, to very near the concentrate channel). For a highly charged membrane, it is a very good approximation to take the straight average of the two values of $c_{\mathrm{T,m}}$ at the two sides of the membrane (still just inside the membrane), i.e., $\left\langle c_{\mathrm{T,m}} \right\rangle = \frac{1}{2}\left(c_{\mathrm{T,m}}|_{\mathrm{d}} + c_{\mathrm{T,m}}|_{\mathrm{c}} \right)$.

How to obtain this total concentration $c_{\mathrm{T,m}}$ at each side? To that end, we return to the earlier Donnan analysis. For a 1:1 salt and no additional partitioning effects, we arrive at

$$c_{\mathrm{T,m}} = \sqrt{X^2 + 4c_{\infty}^2} = |X| + 2\,c_{\infty}^2 \,/\, |X| + \cdots \qquad (70)$$

i.e., this total ions concentration is independent of the sign of X (see full expression), and is always larger than $|X|$, i.e., always $c_{\mathrm{T,m}} \gg |X|$. Now, for a highly charged membrane, with $|X|$ much larger than the two salt concentrations on both sides, we can assume $c_{\mathrm{T,m}} \sim |X|$. That approximation was used in the derivation of Eq. (55) and thus in the final result, Eq. (63), but to be very precise an appropriate average of $c_{\mathrm{T,m}}$ must be used here instead of $|X|$.

The integration of Eq. (68) across the membrane, possible because $J_{\mathrm{m,ions}}$ is independent of position in the membrane, results in

$$J_{\mathrm{m,ions}} = \pm k_{\mathrm{m}} \left(\Delta c_{\mathrm{T,m}} - X \Delta\phi_{\mathrm{m}} \right) . \qquad (71)$$

We calculate λ_{th} according to Eq. (65) by implementing Eqs. (67) and (71), and obtain

$$\lambda_{\mathrm{th}} = 1 - k_{\mathrm{m}} F \Delta c_{\mathrm{T,m}} \,/\, |I| \qquad (72)$$

where we made the replacement $\left\langle c_{\mathrm{T,m}} \right\rangle \to |X|$.

At high enough $|X|$ (relative to c_{c} and c_{d}), from Eq. (70) we can derive that the difference in $c_{\mathrm{T,m}}$ across the membrane can be simplified to $\Delta c_{\mathrm{T,m}} = 2\left(c_{\mathrm{c}}^2 - c_{\mathrm{d}}^2 \right) / |X|$, a result that we can implement in Eq. (72) to arrive at

$$\lambda_{\mathrm{th}} = 1 - \frac{2 k_{\mathrm{m}} F}{|X||I|} \left(c_{\mathrm{c}}^2 - c_{\mathrm{d}}^2 \right) \qquad (73)$$

which is the final equation that we need to solve the full co-current ED model. Let it be reminded that all parameters such as fluxes and potentials in Eq. (71) and other equations for membrane transport all depend on position z in the module, or alternatively, depend on time t^*.

Eq. (73) is interesting in its own right, as it shows that λ_{th} will be high, near unity, at high currents and a high membrane charge, and for low salt concentration differences, but λ_{th} will go down for lower currents and lower membrane charge. It also goes down when k_{m} goes up, which occurs when the membrane thickness is reduced. Indeed, for very thin membranes, ED does not work, because then there is a large flux of coions across the membranes that opposes desalination [42]. (The same problem is found in 'reverse electrodialysis' with membranes that are too thin or too permeable or not charged high enough: then there is a large salt flow across the membranes, so the potentially large power is not realized because the salt solutions in the two channels are rapidly mixed up.) Eq. (73) illustrates that λ_{th} will depend strongly on position in the cell, because current I will change with z, and concentrations c_{d} and c_{c} as well. So current efficiency is not a fixed number, it is not a property of the membranes.

Calculation results are made with this model for co-current flow in ED for a constant V_{cp} across the cell pair (the same value of V_{cp} at each position z). Results show that while the d-channel is desalinating,

the Donnan potential strongly increases on the diluate side (by a value which exceeds the decrease on the concentrate side), the current goes down, and current efficiency decreases, finally to drop all the way to zero, i.e., $\lim_{z\to\infty} \lambda_{\mathrm{th}} = 0$, see Fig. 8. We can use this result to calculate from Eq. (73) the final salt concentration in a single-pass co-current ED cell pair when the cell is large enough, together with Eqs. (52) and (63). These three equations can be solved analytically when we start with a certain final diluate concentration, c_{d}, then calculate c_{c}, then $|I|$, and finally V_{cp}. Calculation results are presented in Fig. 9A and show the final, i.e., minimum, c_{d} that can be reached in an ED stack as function of cell pair voltage V_{cp} for two values of water recovery, WR. Also the current density in this 'steady-state' limit is plotted. In all cases the stack is fed with artificial seawater, i.e., a 0.5 M 1:1 salt solution. Other parameters are $X = 4.0$ M, $k_{\mathrm{m}} = 1$ µm/s, $k_{\mathrm{ch}} = 5$ µm/s, and $L_{\mathrm{ch}} = 200$ µm.

The calculation just discussed describes how deep we can potentially desalinate as function of cell pair voltage, and what will be the final, 'steady state', current density. But it does not give us the average current density, which we need to calculate the electrical energy input. To that end we analyze the full model and for a certain residence time t^* and specific area $a_{\mathrm{d}} = 1/L_{\mathrm{ch}}$, we calculate as function of V_{cp} the exit value for c_{d}, and the average current density $\left\langle I \right\rangle$ (in A/m²). This calculation, of which results are presented in Fig. 9B, also shows a result familiar in the ED literature, that with increasing $\left\langle I \right\rangle$, at some point V_{cp} diverges. This divergence is generally attributed to concentration polarization (CP), which in the context of ED is the *decrease* of salt concentration towards the membranes in the diluate channels. Interestingly, we also find the same divergence in the present model that does not include the CP effect yet. In this model the reason for the divergence of the voltage is that we reach complete desalination, and as a consequence the resistance in the diluate channel rapidly increases just as the Donnan potentials at the diluate-membrane interfaces. We discuss a more extensive 3D ED model including concentration polarization in Section 6.5.

In summary, the co-current ED model is a powerful and insightful model to discuss and quantify several well-known observations in ED, such as the decrease of the current density and current efficiency between inlet and outlet of a flow channel, see Fig. 8. In the next section we use the model to relate stack energy efficiency η_{ED} to the specific productivity of freshwater in ED, a relation that we need in a full cost optimization study.

### 4.2. Energy efficiency and cost optimization of an ED stack

With an ED model available, we can now address the question how to decide at what current to run an ED stack, and how much membrane area to use. To that end we must balance energy and material costs, similar to what we did for RO in Section 3.6. We again set up a relationship between energy efficiency, now given by the symbol η_{ED}, and the volume flow rate of product water per unit membrane area, expressed as a specific productivity, SP, see Fig. 10. In ED electric energy is the main input of energy, given by the product of cell pair voltage and average current density, and thus energy efficiency is given by

$$\eta_{\mathrm{ED}} = \frac{\phi_{\mathrm{v,d}} E_{\mathrm{min}}}{\left\langle I \right\rangle A V_{\mathrm{cp}}} \qquad (74)$$

where A is the area of one of the membranes in a cell pair. Just as for RO, also for ED we set up an equation for the total costs per time of operation, TC, and this equation is basically the same as Eq. (45), now given by [44]

$$\mathrm{TC} = m_1\,\mathrm{CUE}\,\left\langle I \right\rangle A V_{\mathrm{cp}} + m_2 \sum_j \mathrm{CMP}_j A_j / \Delta t_j \qquad (75)$$

which has the costs of electrical energy as a first contribution, and second a summation over AEMs and CEMs of a term that includes
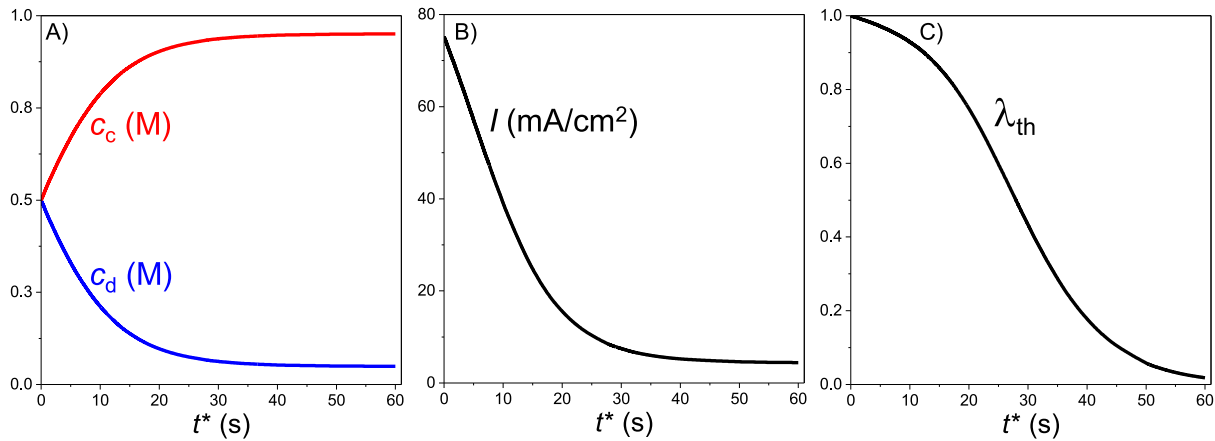
Fig. 8. Calculations of desalination in electrodialysis with co-current flow in diluate and concentrate channels for V_{cp} = 180 mV, c_f = 0.5 M, WR = 0.5, and X = 4.0 M. As function of time-on-stream, t^*, salt concentrations in the two channels change, first rapidly, then slowly, while current I goes down as well as current efficiency, λ_{th}. In steady-state (at large t^*), there is still a flow of current across the channels and membranes, but the net salt transport is zero, thus $\lambda_{th} \to 0$.
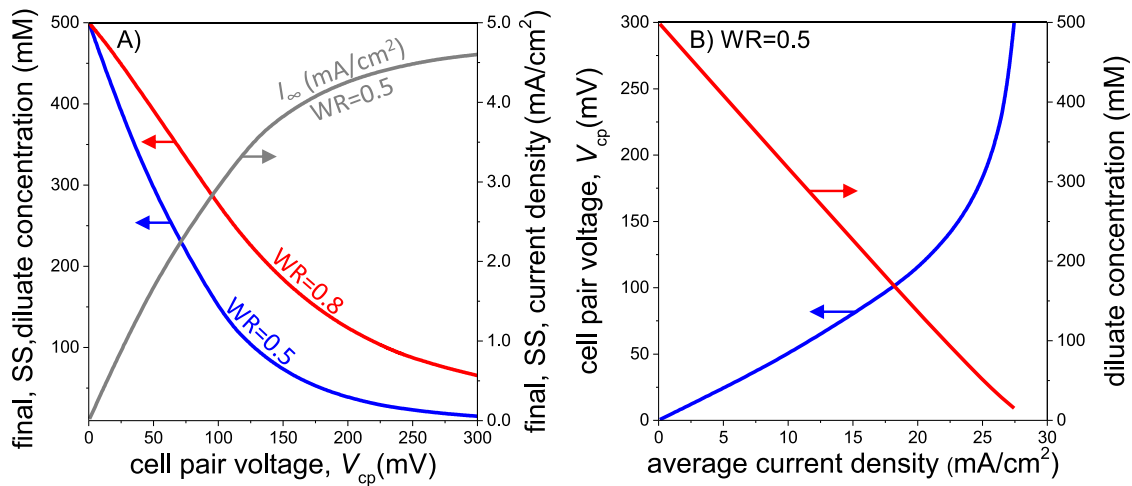
Fig. 9. Analysis of concentrations and current density in ED based on co-current flow. (A) For two values of WR we analyze as function of V_{cp} the steady-state diluate concentration, c_d, which can be reached after a long enough residence time t^*, as well as the resulting final current density for WR = 0.5. (B) For a fixed t^* = 40 s (SP = 5), the cell pair voltage V_{cp} diverges at a certain average current density $\langle I \rangle$, when desalination goes to completion.

their purchase costs per m^2, their area, A_j, and their lifetime, Δt_j. We now assume that all three of these factors are the same for the two membranes. We insert Eq. (74), divide by $\phi_{v,d}$, multiply by the membrane transfer coefficient, k_m, and obtain

$$\text{tc} = \frac{\alpha \cdot \text{ec}_{\min}}{\eta_{ED}} + \frac{1}{SP} \quad , \quad \alpha = \frac{m_1 \cdot \text{CUE} \cdot \Pi_f \cdot \Delta t_j \cdot k_m}{2 \cdot m_2 \cdot \text{CMP}} \tag{76}$$

where $SP = \phi_{v,d}/\left(A k_m\right)$. We can minimize η_{ED} if we know its dependence on SP, for a given value of α. Based on the co-current ED model, we can generate a list of calculation outputs for a specific membrane system, which are the 'data points' in Fig. 10, and fit with an equation that subsequently is used in the cost optimization study. Interestingly, the same as for RO, see Fig. 6, we obtain a curve of η vs. SP with a maximum efficiency at low SP, and a decrease in η at higher SP. Here, the blue fit line in Fig. 10 follows the trend $\eta \propto (SP+cnst)^{-1}$, while a more accurate fit line (green) is obtained by 'multiplying the blue line' with an empirical function, tanh(SP$^{0.8}$/3.2). These functions do not need to have a physical basis; they are just fit functions that 'summarize' real calculation results in a continuous function that can be used in a cost optimization study. When the purchase costs of membranes go down, this minimization shows that we should run at lower SP, i.e., for a given production of freshwater we should install more membranes, and run them at a higher efficiency. Thus one can

again quip that 'cheaper membranes are more efficient' just as was the case for RO.

5. Fundamentals of ion and water transport across membranes

5.1. Introduction

In the previous sections we made use of simplified approaches for the transport of solutes and water through RO and ED membranes. In the RO-calculation we neglected charge effects, while in the ED-model we neglected ion–membrane friction and advection of ions. In a generalized approach all these driving forces and frictions are jointly considered, in both types of processes. Also the acid–base reactions between ions, often also involving the H$^+$-ion, are important to include. On both outsides of the membranes there is equilibrium (across the interface) both with regard to pressure (mechanical equilibrium), and with regard to chemical potential of solutes (chemical equilibrium). These equilibria also depend on non-electrostatic contributions to the partitioning of solutes across the water–membrane interface of which the two most important ones are affinity and volumetric excess effects [5]. For transport across the membrane, be it for membranes as thin as 100 nm as in RO, and membranes 100 to 1000 times thicker for ED, we can start with continuum theory from the field of electrokinetics
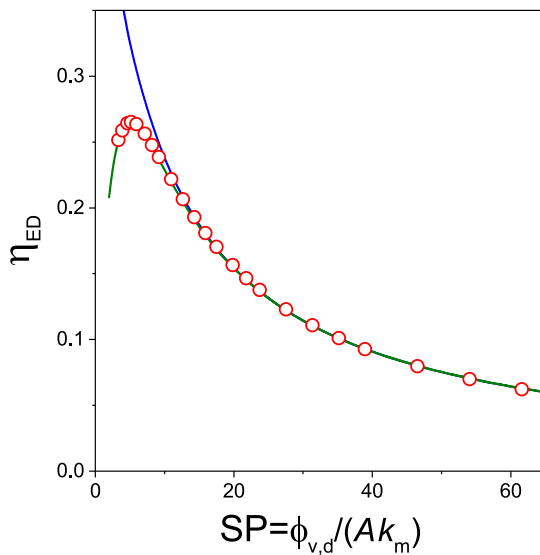
Fig. 10. Energy efficiency in electrodialysis, η_{ED}, versus specific productivity, SP, according to the co-current ED model for the situation analyzed in Figs. 8 and 9 (red circles). In all calculations a 500 mM salt solution is desalinated to 50 mM, and water recovery is 50%. Fit line according to $\eta \propto (\text{SP}+\text{cnst})^{-1}$ (blue) and more accurate fit (green line) can be used in cost optimization studies.

of thin channels, and apply this theory to transport in the pores in RO and ED membranes. These models, such as the space charge (SC) model [45–49], then become much more simple because profiles in concentration and potential across the cross-section of a pore in the membrane then do not need to be considered. This simplified 'uniform potential' (UP) model, i.e., the SC-model with averaging over the cross-section of the pore, describes ion transport and water flow through the pores of a membrane, and considers the effect of pressure on both membrane interfaces [32,49–51]. The UP-model is thus an extension of the Teorell–Meyer–Sievers (TMS) model that describes ion transport across membranes, but TMS theory does not include water flow. The UP-model can now be extended to incorporate many more effects than we could in the SC model. Besides water–membrane and water–ion friction, we can now also include ion–membrane friction and ion–ion friction, the latter describing how ions that overtake slower ones drag these along, and vice-versa slow ions will retard faster ones. In the two-fluid model (TFM) [52,53] this detailed model that includes various frictional forces is extended with a description of water flow [54,55].

In the two-fluid model, a local force balance acting on solutes (such as ions) includes driving forces and frictions. Driving force acting on a solute are mathematically formulated as the negative of a gradient of an ion's chemical potential. Frictions experienced by a solute are with the water flowing through the pores, and with the membrane matrix, which is an immobile background structure. For the water a similar force balance is set up but driving forces acting on the water are hydrostatic and osmotic pressures gradients [36,38]. Thus ions and other solutes are described in a very different manner from how the water that flows past the ions through the pores is described. This is one of the key points of the two-fluid model (TFM). And this is different from Maxwell–Stefan (MS) theory that was successfully developed for multicomponent gas flows in porous media where all gas substances can be described in like fashion. This MS theory has also been applied to electrolytes, i.e., the flow of ions and water through porous media, but it then faces several shortcomings. MS theory applied to electrolyte flow relies quite heavily on a statistical–mechanical view wherein the molecular nature of water is included and all ions and other solutes just like each water molecule occupy one of the available statistical sites. This electrolyte version of MS theory also too much considers water to flow according to its own concentration gradient,

as if it is also a dispersed species, which it is not. Instead, water molecules in a porous medium aim to 'keep contact' with as many water molecules as possible, and thus across the membrane they will fill up all available space forming thin 'strands' of connected water pathways. Thus the water in a membrane is not present in a dispersed 'gas-like' state, but is a cohesive continuum fluid that fills up the porous medium. Ions and other solutes – these are discrete, dispersed entities – they travel across these pathways formed by the water molecules. MS theory applied to electrolytes does not consider the difference between total, hydrostatic and osmotic pressure, and generally has a hard time implementing partitioning and equilibrium conditions on the outer surfaces of membranes. Instead, all of these effects are comprehensively included in the two-fluid model, which describes the flow of ions and other solutes through tortuous media simultaneously with solvent flow, using different expressions for both. We will demonstrate the accuracy of the two-fluid model by comparing with results of an experiment where water and solutes flow in opposite directions through an ion-exchange membrane (osmosis), which is an experiment that is very hard to describe precisely. But first we present the basics of flow of ions (and other solutes) and water according to the two-fluid model.

5.2. Flow of solutes through membranes in the two-fluid model (TFM)

To describe the flow of ions through a porous tortuous medium, we first of all set up an expression for the chemical potential of an ion. Ions can be hydrated to some extent, and the water molecules that are firmly bound in its water shell are part of what we call the ion. In this section the porous medium is a membrane, so at some point the explanation switches from 'porous medium' to 'membrane.' We can consider multiple contributions to the chemical potential of an ion (unit J/mol) in a porous medium, adding up to

$$\mu_i = \mu_{\text{ref},i} + RT \left(\ln c_i + z_i \phi \right) + \mu_{\text{aff},i} + \mu_{\text{exc},i} + v_i P^{\text{tot}} \cdots \quad (77)$$

where the reference value $\mu_{\text{ref},i}$ of importance when ions take part in chemical reactions, while $\ln c_i$ relates to diffusion (ion entropy), $z_i \phi$ to electrostatic effects, $\mu_{\text{aff},i}$ to an affinity, leading to (one contribution to) a solubility S_i or partitioning coefficient Φ_i, and where finally $\mu_{\text{exc},i}$ is a function that describes various volumetric interactions between ions, and between ions and the porous medium [17]. The pressure insertion term $v_i P^{\text{tot}}$ relates to the molar volume of an ion v_i, where total pressure P^{tot} is hydrostatic pressure, P^{h}, minus osmotic pressure, Π.

Across any thin interface, where we can assume mechanical equilibrium, the total pressure is invariant, as we will discuss in Section 5.3, so in a partitioning function, as below, this term cancels out. For the volumetric term, $\mu_{\text{exc},i}$, when only interactions of an ion with the porous medium are of importance (and not between ions), then it is a constant factor that can then be jointly considered with $\mu_{\text{aff},i}$. Then, for a neutral solute, we arrive for the distribution of a solute across a porous medium/solution interface (between 'in' and 'out'), at

$$\frac{c_{i,\text{in}}}{c_{i,\text{out}}} = \exp\left(- \left(\mu_{\text{aff},i} + \mu_{\text{exc},i} \right) / RT \right) = S_i = \Phi_i \quad (78)$$

where the solubility S_i or partitioning coefficient Φ_i is a constant factor if the affinity and excess terms do not depend (too much) on concentrations just outside and inside the pore. Also other effects can contribute to Φ_i which then leads to additional thermodynamic penalties (or attractions) for an ion to enter a porous medium. The excess contribution is often described as function of an ion size–pore size ratio, λ, described for a perfectly cylindrical pore and spherical ions by $\Phi_i = \left(1 - \lambda_i \right)^2$, but many more accurate expressions are available [39]. For ions, with a charge different from zero, we can extend Eq. (78) with a Boltzmann (Donnan) term, and we then end up with

$$c_{i,\text{in}} = c_{i,\text{out}} \Phi_i \exp\left(-z_i \Delta\phi_{\text{D}} \right) \quad (79)$$

which extends Eq. (57), by now including a partitioning effect that has a non-electrostatic origin.

In the two-fluid model, on the basis of Eq. (77) we describe the driving forces acting on an ion as minus the gradient of chemical potential. And these driving forces are compensated by all frictional forces, according to a force balance given by

$$\mathcal{F}_{\text{driving},i} + \mathcal{F}_{\text{friction},i} = 0. \tag{80}$$

Assuming for simplicity ions not to have volume, thus $v_i = 0$, we obtain for the driving force acting on a mole of ions

$$\mathcal{F}_{\text{driving},i} = -\frac{\partial \mu_i}{\partial x} = -RT \left(\frac{1}{c_i} \frac{\partial c_i}{\partial x} + z_i \frac{\partial \phi}{\partial x} \right) \tag{81}$$

where we consider a single coordinate, x. An extension to multiple coordinates or dimensions is straightforward. We can leave out here a gradient-term related to $\mu_{\text{aff},i}$ because this ion–membrane affinity will be invariant across the membrane. And for the same reason we also leave out the excess-term that relates to volume effects. Thus we only have to consider a force related to diffusion, and to the electric field, i.e., electromigration.

Frictional contributions are due to friction of the ion with other ions that have a different velocity (otherwise there is no friction), with the water, and with the membrane matrix. Friction with other types of ions depends on the concentration of those other species, i.e., the more of them, the more friction, but the friction with the water, and with the membrane matrix, these terms have no dependence on concentration. We neglect ion–ion friction now – otherwise see Ref. [54] – so the friction of ions is only with the water that also flows through the porous medium, and with the membrane matrix. Each frictional term is the product of the velocity difference and a friction factor describing friction of the ion and that other phase. We then arrive at (p. 128 in Ref. [38])

$$\mathcal{F}_{\text{friction},i} = -\sum_j f_{i\text{-}j}^* \left(v_i - v_j \right) = -f_{i\text{-w}}^* \left(v_i - v_{\text{w}} \right) - f_{i\text{-m}}^* v_i \tag{82}$$

where water velocity is v_{w} and we included in the last part that the velocity of the membrane is zero, $v_{\text{m}} = 0$. We present here velocities as superficial velocities, per unit total membrane area. In a more detailed analysis we start with interstitial velocities, for instance for the water that is its velocity flowing through the space not occupied by the solutes within the pores of the membrane structure. In that more detailed analysis we also first set up these forces balances in the direction along the flow path of a tortuous pore, and when converting to an x-coordinate that is directed straight across the membrane, a tortuosity factor arises in the final equations. These detailed steps go beyond the scope of this tutorial review, but are explained in Ref. [39].

We can rewrite the ion–water frictional coefficient to a diffusion coefficient of the ion in the membrane, $D_{\text{m},i}$, by the Einstein equation, $f_{i\text{-w}}^* = RT/D_{\text{m},i}$ (p. 128 in Ref. [38]). This diffusion coefficient is lower than in free solution because it includes the porosity and tortuosity of the membrane pores. We now obtain an extended Nernst–Planck equation for ion flow inside a membrane (Eq. (7) in Ref. [5]) where advection, diffusion and electromigration all contribute [56]

$$J_i = K_{\text{f},i} c_{\text{m},i} v_{\text{w}} - K_{\text{f},i} D_{\text{m},i} \left(\frac{\partial c_{\text{m},i}}{\partial x} + z_i c_{\text{m},i} \frac{\partial \phi}{\partial x} \right) \tag{83}$$

and where we also incorporated that $J_i = c_{\text{m},i} v_i$. Concentrations here are those inside the membrane pores. The friction factor, or hindrance function, $K_{\text{f},i}$, is given by $K_{\text{f},i} = 1/\left\{1 + f_{i\text{-m}}^*/f_{i\text{-w}}^*\right\}$, and has a value between 0 and 1, and describes that ions have a direct friction with the membrane structure, not only with the water that directly envelopes them and flows past them. The ion–membrane frictional coefficient is $f_{i\text{-m}}^*$ but its value we do not need to know if we phrase the problem in terms of $K_{\text{f},i}$. In a further extended theory that includes how part of the pore volume is occupied by solutes and not available for the flow of free water, then instead of the unique function $K_{\text{f},i}$, we have two different functions that we could call $K_{\text{c},i}$ and $K_{\text{d},i}$, in line with literature on NF transport theory where often separate 'convective' and 'diffusive' hydrodynamic functions are implemented. But in the

two-fluid model, in case we assume that solutes do not occupy too much space in the pores, there is one friction function, $K_{\text{f},i}$. If $K_{\text{f},i}$ is unity, ions have no friction with the membrane matrix, and then the dependence of water flow on pressure simplifies significantly, with a constant water permeability factor, $k_{\text{F-m}}^*$, which otherwise depends on the local concentration of solutes in the membrane, as we will explain in the next section. In any case, Eq. (83) is a general expression for ion transport in porous media, extended compared to the standard Nernst–Planck equation with advection and with ion–membrane friction, which leads to the factor $K_{\text{f},i}$.

5.3. Flow of water through membranes in the two-fluid model (TFM)

Now we continue with transport of water through the pores of a porous medium. In the derivation that follows, we assume the pores are filled with water completely and ions are 'point charges'. For a full account including solute volume effects, see Ref. [39]. We can now set up a balance of forces acting on a volume element of water in the pore, with the driving force a gradient in total pressure, i.e., $-\partial P^{\text{tot}}/\partial x$ is the force acting on a volume element of water. It indeed has the correct unit N/m^3. The forces acting on the water are a friction with the membrane structure, $f_{\text{F-m}} RT \left(v_{\text{m}} - v_{\text{w}} \right)$, where $v_{\text{m}} = 0$ because the membrane is immobile (ref. [38], p. 126), and friction with all types of solutes, and this friction is proportional to the concentration of that type of solute, which leads to $\sum_i f_{i\text{-w}}^* c_{\text{m},i} \left(v_i - v_{\text{w}} \right)$. All these forces are added up, and their sum-total is set to zero, resulting in

$$-\frac{\partial P^{\text{tot}}}{\partial x} - f_{\text{F-m}} RT v_{\text{w}} + \sum_i f_{i\text{-w}}^* c_{\text{m},i} \left(v_i - v_{\text{w}} \right) = 0. \tag{84}$$

We can solve Eq. (84) at each position in the membrane, together with the extended Nernst–Planck equation, Eq. (83). Now, a significant simplification is arrived at if we assume there is no ion–membrane friction, and thus we can set $K_{\text{f},i} = 1$ in the NP equation, Eq. (84), for all ions. Then inserting the NP equation in Eq. (84) results in

$$-\frac{1}{RT} \left(\frac{\partial P^{\text{h}}}{\partial x} - \frac{\partial \Pi}{\partial x} \right) - f_{\text{F-m}} v_{\text{w}} - \sum_i \left(\frac{\partial c_{\text{m},i}}{\partial x} + z_i c_{\text{m},i} \frac{\partial \phi}{\partial x} \right) = 0 \tag{85}$$

where we implemented that $P^{\text{tot}} = P^{\text{h}} - \Pi$ and $D_{\text{m},i} = RT/f_{i\text{-w}}^*$. Now, because in the ideal case that we discuss here the osmotic pressure equals the total ion concentration times RT, thus $\Pi = c_{\text{T,m}} RT$ with $c_{\text{T,m}} = \sum_i c_{\text{m},i}$, Eq. (85) simplifies to

$$-\frac{1}{RT} \frac{\partial P^{\text{h}}}{\partial x} - f_{\text{F-m}} v_{\text{w}} + X \frac{\partial \phi}{\partial x} = 0 \tag{86}$$

and thus we have an exact cancellation of the osmotic pressure acting on the water, and the diffusional forces acting on the ions, which transfer to the water via ion–water friction. But this only happens when the ions have no friction with other phases except for the water. In Eq. (86) we also included local electroneutrality in the membrane, $\sum_i z_i c_{\text{m},i} + X = 0$ (with X either positive or negative). Then we end up with Eq. (86) where we have a hydrostatic pressure gradient acting on the water, water–membrane friction, and an electrostatic body force term, which actually entered this force balance because of water–ion friction. We can rewrite Eq. (86) to

$$v_{\text{w}} = -\Bbbk_{\text{F-m}} \left(\frac{1}{RT} \frac{\partial P^{\text{h}}}{\partial x} - X \frac{\partial \phi}{\partial x} \right) \tag{87}$$

where we made the replacement $\Bbbk_{\text{F-m}} = 1/f_{\text{F-m}}$. For an uncharged membrane, $X = 0$, and then Eq. (87) simplifies to the Darcy equation, Eq. (34). Thus water flows across an uncharged membrane not by diffusion but because of an internal pressure gradient [26,31,57,58]. Thus, Eq. (87) is an extension of Darcy's law, valid for charged porous media [28,50]. For a constant membrane charge, it can be easily integrated between the two sides of the membrane. Let it be reminded that the last three equations all assumed $K_{\text{f},i} = 1$.

The final element of transport theory through a porous structure filled with a continuum fluid such as water, with dispersed enclosed entities, such as ions, is mechanical equilibrium at the interface between

the structure and the outside solution. This was already discussed in Section 3. Here we derive the mechanical equilibrium condition based on Eq. (85), because with all gradient terms much larger in a thin interfacial region than the terms proportional to velocities (or in other words, the structure of the interfacial region is not significantly modified by flows of ions and water across it), we arrive at the conclusion that P^{tot} is invariant across any thin interface, and thus $P^{\text{h}} - \Pi$ is invariant as well [32,45,50], and this leads to the earlier conclusion that across an interface the change in osmotic pressure Π (either up or down) equals the change in hydrostatic pressure P^{h} across that same interface. It may be good to reiterate that osmotic pressure is not really a pressure in the sense that it has a direct 'hydraulic' or 'mechanical' impact. It is simply a measure of solute concentration, in the ideal case linearly related to solute concentration.

This analysis allows us to address the question why water always has a tendency to flow to that side of a membrane that has the highest salt concentration. This is because of the two osmotic pressure changes across the two outer surfaces, and they are different if the outside solutions are different [57,59]. And both for the case of neutral solutes and an uncharged membrane, and for the case with ions and a charged membrane, in both cases this leads to a hydrostatic pressure profile in the membrane that is such that water will flow to the concentrated side [58]. For a neutral membrane the osmotic pressure goes down the most on the high-concentration side, and thus hydrostatic pressure there drops the most as well (from a value outside the membrane). For a highly charged membrane (and when Φ_i is not too far from unity), osmotic pressure goes up upon entering the membrane. This increase in pressure is the lowest on the high-concentration side, at a value just above the charge density $|X|$. Thus again we develop a pressure profile inside the membrane that pushes the water to the high-salinity side. All of this assumes the two outside hydrostatic pressure to be the same, or close to one another. If not, if we apply a hydrostatic pressure difference across the membrane, we can overcome the osmotic effect, and this is of course what we do in RO and NF.

5.4. Counterfluxes of salt and water in osmosis

To illustrate the two-fluid model, and to provide evidence for its validity and accuracy, we discuss results of an accurate fit of this theory to data of the flow of water and salt across an ion-exchange membrane. This experiment is called osmosis, and water and salt flow because of a difference in salt concentration between the two outside solutions on either side of the membrane, without pressure differences or current. Results of this experiment are presented in Fig. 11 as function of the concentration on the low-salinity side, c_{d}, which has values changing (in time) from 4 mM to 130 mM. During that time the salt concentration on the concentrate side decreases from 800 to 525 mM. Over the 35 hr of the experiment, the volume on the diluate side drops by 40% and that water flows to the concentrated side, see Ref. [39] for details. In this experiment water flows to the high-salinity side, while salt flows in the other direction. Thus, inside the membrane these two flows are in opposite direction. This makes this an experiment that is not easy to accurately reproduce in a theoretical model, i.e., it is a very good test of a mass transfer theory.

When we apply the mass transport theory described above, with cation and anion fluxes the same (which is because the electrical current through the membrane is zero), and with equal diffusion coefficients of the ions in the membrane, we find that it works excellently and results in the very good fit to the data shown in Fig. 11. In the integration of the water force balance, Eq. (84), the total concentration of ions in the membrane is set to a constant value, which is calculated as an average of the values on the two sides, and these concentrations are calculated by Eq. (70). The salt flux is given by an equation that we will discuss further on, Eq. (91). Based on Ref. [60] we derive a value of

$\Phi_i = 0.82$. The partitioning function Φ_i is part of the calculation of $c_{\text{T,m}}$, by making use of Eq. (79) which is evaluated for both ions, leading to

$$c_{\text{T,m}} = \sqrt{X^2 + \left(2\Phi_i c_\infty\right)^2} . \tag{88}$$

Membrane charge density is $X = -5.1$ M and membrane thickness is $L_{\text{m}} = 120$ μm. To fit the model to the data, we derive a hindrance factor of $K_{\text{f},i} = 0.51$. Because $K_{\text{f},i} \neq 1$, we cannot use Eq. (87). The values we derive for the transport parameters $k_{\text{m}} = 0.31$ μm/s (corresponding to a diffusion coefficient in the membrane about 50× less than in free solution), and $k_{\text{F-m}} = 137$ (mm)^4/mol/s (which corresponds to ~20 mL/m^2/hr/bar) are in line with earlier reported values in Ref. [54]. Thus, we can conclude that the two-fluid model including chemical and mechanical equilibrium is very well capable of describing fluxes of water and salt in the osmosis experiment. Note again that these fluxes were in opposite directions inside the membrane.

It is interesting to estimate the velocities of the water and the ions in the membrane. We assume a porosity of 34% and we consider velocities straight across the membrane. We analyze the start of the experiment, when the concentrations on the two sides are 4 mM and 800 mM. The water velocity is now ~300 nm/s. The counterion velocity is constant across the membrane and is ~15 nm/s. This is a velocity in the direction opposite to the water flow and it is about 5% of the water velocity. Thus the counterions first of all have a velocity relative to the water, to not be dragged along, and then a 5% extra velocity to make them move against the water in the reference frame of the membrane. The coions have a concentration that on the high-salinity side is about a factor of 100 smaller than that of the counterions, and many orders smaller than that on the low-salinity side. If velocity is calculated as a flux divided by a concentration, one could state that the velocity of the coions is much higher than of counterions, and rapidly increasing towards the low-salinity side. But if coions are predominantly transported by diffusion, this interpretation of velocity must not be taken too literally — it is not the case that an individual coion accelerates while moving across the membrane [61].

6. Extended models for reverse osmosis and electrodialysis

6.1. 1D RO model for electrolyte solutions based on good coion exclusion

In this and the next section we focus on RO for a 1:1 salt solution and a charged membrane, using a model based on the assumption that coions are excluded very well from the membrane and thus the salt flux (we have equal fluxes of cations and anions, all denoted by J_i in this section) is determined by the transport rate of the coions. For a highly charged membrane (relative to $\Phi_i c_\infty$), we have an abundance of counterions and only a few coions in the membrane, and then according to the extended Nernst–Planck equation the transport rate of a 1:1 salt with equal ion diffusion coefficients and equal values of $K_{\text{f},i}$ and Φ_i is given by

$$J_i = 2 \cdot v_{\text{w}} \cdot |X|^{-1} \cdot K_{\text{f},i} \cdot \Phi_i^2 \cdot c_{\text{int}} \cdot c_{\text{p}} \cdot \frac{\sinh\left(v_{\text{w}}/k_{\text{m},i} + \ln\left(c_{\text{int}}/c_{\text{p}}\right)\right)}{\sinh\left(v_{\text{w}}/k_{\text{m},i}\right)} \tag{89}$$

which is Eq. (32) in Ref. [32] and Eq. (41) in Ref. [53], extended to include the term $K_{\text{f},i}\Phi_i^2$. Implemented here is an expression for the coion concentration just in the membrane relative to that outside, $c_{\text{m,co}} \cdot |X| = \left(\Phi_i c_\infty\right)^2$, valid when $|X| \gg \Phi_i c_\infty$. In Eq. (89), 'int' refers to a position on the upstream side just outside the membrane. For low water flow rates, Eq. (89) simplifies to

$$J_i \cdot \frac{|X|}{K_{\text{f},i}\Phi_i^2} = k_{\text{m},i}\left(c_{\text{int}}^2 - c_{\text{p}}^2\right) + v_{\text{w}}\left(c_{\text{int}}^2 + c_{\text{p}}^2\right) + \cdots \tag{90}$$

which has a term dependent on $k_{\text{m},i}$ (thus based on diffusion), and a second term proportional to v_{w} (advection). At low enough v_{w} only the first, diffusional, term plays a role, and then salt flux does not depend
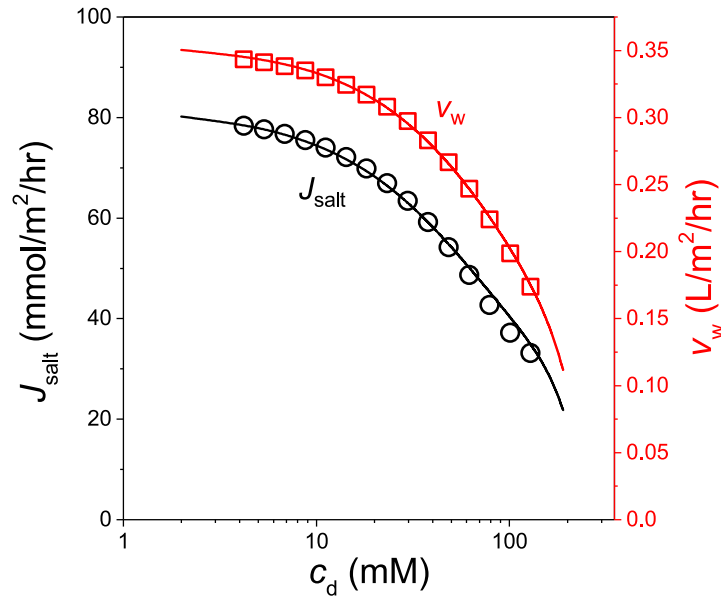
Fig. 11. Experimental and theoretical results of salt flux, J_{salt}, and water velocity, v_w, across a cation-exchange membrane placed between two solutions with different salt concentration (initially $c_d = 4$ mM and $c_c = 800$ mM). Water flows to the high-salinity side, and salt in the other direction. There is no external pressure difference and there is no current. See main text for parameter settings.

on v_w. However, advection starts to play a role when v_w is of the order of $k_{m,i}$. If we only use the first term in Eq. (90), we arrive at

$$J_i = B' \cdot RT \cdot \left(c_{int}^2 - c_p^2 \right) \tag{91}$$

where B' is a salt permeability with unit m/(s·Pa) given by

$$B' = \frac{K_{f,i} \, k_{m,i} \, \Phi_i^2}{|X| \, RT} \tag{92}$$

which can be recalculated to a number with dimension LMH/bar by multiplying with $3.6 \cdot 10^{11}$ (where LMH refers to liters of permeate water per square meter of membrane per hour). We include the CP layer, and we can thus describe c_{int} by Eq. (31). If we assume a high retention and thus $c_p \ll c_f$, this simplifies to

$$c_{int} = c_f \cdot \exp\left(v_w / k_{dbl,i} \right) \tag{93}$$

where we assumed that beyond the DBL the salt concentration is c_f (i.e., we consider the limit of low water recovery). Salt retention is then given by

$$R_i = 1 - B' \cdot RT \cdot c_f \cdot v_w^{-1} \cdot e^{2 \, v_w / k_{dbl,i}} \tag{94}$$

which predicts that retention not only depends on permeate water flux, v_w, but also on feed concentration, as is well-known experimentally [62]. This is different in the SD-model where the latter dependence is absent.

To calculate the pressure drop across the membrane we can use Eq. (84) which results in

$$\frac{1}{RT} \frac{\partial P^{tot}}{\partial x} + f_{F\text{-}m} v_w + \frac{1}{D_{m,i}} \left(c_{T,m} v_w - 2 J_i \right) = 0 \tag{95}$$

when we assume equal diffusion coefficients of the two ions in the membrane. If we insert that $c_{T,m} \sim |X|$ and $J_i = c_p v_w$, we arrive at an expression that can be integrated across the membrane, after which the pressure term can be evaluated on both sides ($P^{tot}\big|_L = P^{h,L,\infty} - 2RT c_{int}$, $P^{tot}\big|_R = P^{h,R,\infty} - 2RT c_p$, and $\Delta P^{h,\infty} = P^{h,L,\infty} - P^{h,R,\infty}$), which leads to

$$\Delta P^{h,\infty}/RT - 2 \cdot \left(c_{int} - c_p \right) = v_w \cdot \left(f_{F\text{-}m} L_m + \left(|X| - 2c_p \right) / k_{m,i} \right) \tag{96}$$

which can be analytically solved. In practice, it will be hard to distinguish the various resistance terms on the right, and it is useful to

simplify and obtain for the permeate water flux

$$v_w = A \cdot \left(\Delta P^{h,\infty} - \Delta \Pi^\infty \right) \tag{97}$$

with A an effective water–membrane permeability with unit m/(Pa.s), or LMH/bar, and where the osmotic pressure across the membrane, $\Delta \Pi^\infty$, is given by $\Delta \Pi^\infty = 2 RT \left(c_{int} - c_p \right)$. This equation is the same as in the SD-model, but the derivation is different. In Fig. 12 we evaluate Eqs. (94) and (97) for three feed concentrations of a 1:1 salt to describe salt retention R_i and water flow rate v_w. We use $k_{dbl,i} = 65$ LMH, $A = 1.70$ LMH/bar, and $B' = 10$ mLMH/bar. Detailed comparison with data [33,63] leads to the conclusion that $|X|$ scales with c_{int} to the power 0.4. Implementing this effect leads to a salt permeability B'' that is an intrinsic membrane property.

6.2. 2D RO model for electrolyte solutions in the good coion exclusion regime

We continue with a discussion of RO with ideal 1:1 salt solutions and present results of a 2D module calculation. This can later be extended to solutions of more ions, and effects of pH on ion protonation and on membrane charge (acid–base reactions) [14,55,64–67]. We use a membrane transport model where coion diffusion is the limiting transport step, described by Eqs. (91), (93), and (97). We also include a CP-layer (DBL) as boundary equation. Concentration c_f in Eq. (93) becomes a z-coordinate dependent upstream salt concentration.

We implement these equations in a 2D model for an RO module similar to the approach for neutral solutes in Section 3, where we solved transport equations at each position ξ in a module, which led to the calculation results presented in Fig. 6. We use the same approach and analyze a module with a given membrane area, and always the same average permeate water flux that we set to a realistic value of 20 LMH with a feedwater concentration c_f either of 50 or 500 mM, representative of moderately brackish water, and of seawater. In both cases there is a minimum pressure and one could in theory work just beyond that pressure. Then water recovery is very low and we have a very low permeate concentration, see Fig. 13A. However, this choice leads to a very high energy cost per unit produced water because a lot of feedwater needs to be pressurized, see Fig. 13B. It is better to
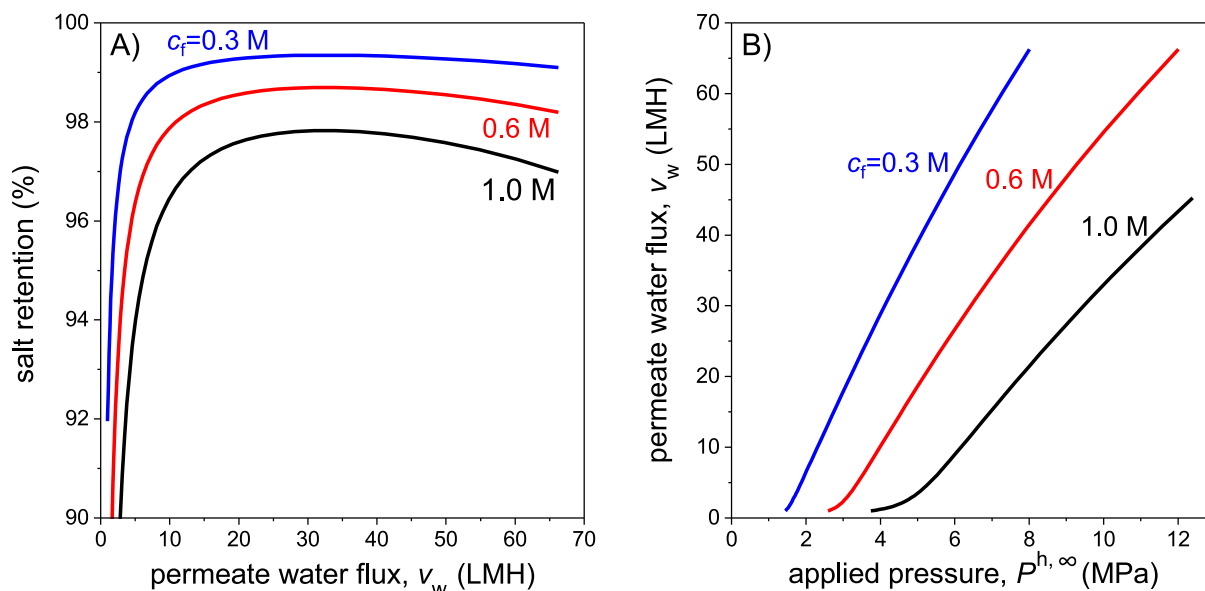
Fig. 12. Calculations for desalination of a 1:1 salt solution in reverse osmosis. (A). Salt retention as function of permeate water flux v_w and feed salt concentration c_f. (B). Dependence of v_w on applied pressure, $\Delta P^{h,\infty}$. Calculations based on Eqs. (94) and (97).

increase the applied pressure and increase water recovery. We then need less feedwater, still producing 20 LMH permeate, while c_p only changes moderately. The energy costs decrease and thus the total costs of operation, TC, as well, until a minimum is reached beyond which TC goes up again. We use Eq. (45) to describe the cost of operation of the RO module. Because of the fixed system size, the second part related to membrane costs is constant, and thus, to find the optimum pressure and other factors, various cost factors such as CUE are irrelevant as well. The only thing of importance in the present calculation is the applied pressure, $\Delta P^{h,\infty}$, times the feed flow rate $\phi_{v,f}$ (which is proportional to the fixed production flowrate, divided by WR) and times the factor $1 - \eta_{ERD}(1 - WR)$, where we use $\eta_{ERD} = 0.5$. We leave out other cost factors relating to pretreatment or brine discharge.

For $c_f = 50$ mM, this simple calculation provides a minimum in total costs at a pressure around 19 bar (about 25% above the minimum pressure), and a water recovery at that condition of WR $\sim$ 78%. For seawater, $c_f = 500$ mM, the minimum pressure is at $\sim$46 bar, the optimum is at 64 bar (about 40% above the minimum), and water recovery at that optimal condition is 55%. Interestingly, this water recovery, in the range 50%–60%, is a common value for operation of seawater desalination plants.

When we compare these two conditions of c_f 50 mM and 500 mM, we have for the same water flowrate v_w a much better retention for brackish water than for seawater (when we define 'goodness' as how close we are to 100%). Indeed, for brackish water we have at the economic optimal point a permeate concentration of $c_p = 0.30$ mM and thus a retention of $\sim$99.4%, while for seawater we have at the optimum a permeate concentration of $c_p \sim 14$ mM, and thus a retention of $R_i \sim 97\%$. This is about a factor of 6 difference (based on how far we are from 100%).

6.3. 2D cross-current ED model

We continue with advanced calculations for electrodialysis (ED). In Section 4 a model for ED was discussed where the water flows co-currently along the membranes. (Note that 'current' in a description of flow patterns does not relate to electrical currents, but to the direction of the flow of water in the channels.) In the present section we compare this flow pattern with two other modes of water flow. The first

alternative is counter-current operation as explained in Fig. 14. This is mathematically similar to co-current flow, but now the direction of water flow in the concentrate channels is opposite to that in the diluate channels. Finally we compare with cross-current flow, where flow in the concentrate channels is 'at a 90 degrees angle' relative to the flow direction in the diluate channels. Mathematically, a two-dimensional (2D) problem is then solved. We compare ED operation in these three modes on the basis of the important curve of efficiency η_{ED} vs. specific productivity, SP. So each calculation is made for the same separation, where the diluate concentration goes down from 500 mM to 50 mM, and water recovery is 50%. As Fig. 14 demonstrates, efficiency is best (for a certain value of SP) in counter-current operation, next best is cross-current, and last is co-current flow. The differences are significant in a range of SP-values between $\sim$ 3 and 10. And in addition, because it is never useful to work 'left of' the maximum, for co-current flow one would not operate below SP $\sim$ 5, while for counter-current flow it can still be sensible to operate as low as SP = 3. Thus, in this range of SP-values, there is a significant effect of the flow geometry on operational efficiency. However, for higher production rates, in this case beyond SP $\sim$ 15, the three flow geometries all give the same result, i.e., the exact type of flow does not matter at these high flow rates. The flow geometry only matters at low SP, and as discussed before, operation at low SP is economically attractive when material costs are low relative to energy costs [44]. When instead costs of materials are a large part of the total operational expenses, operation is at an economic optimum with less membrane area, at higher electrical currents, and then calculation results are that the dependency of efficiency on productivity does not depend very much on the mode of operation.

6.4. Optimization of a stack of two ED modules

Now we extend the calculation for ED to the multi-module level. A layout is considered with two ED modules (two ED stacks) that can be different from one another, and together they are the ED system. We consider different ways to combine these two modules in the system. We make comparisons for the same value of SP evaluated at the system-level. Thus, we add together all areas in the two modules to a total area A that is used in the calculation of SP, and if we compare with a system consisting of a single module, that one module can have the same total
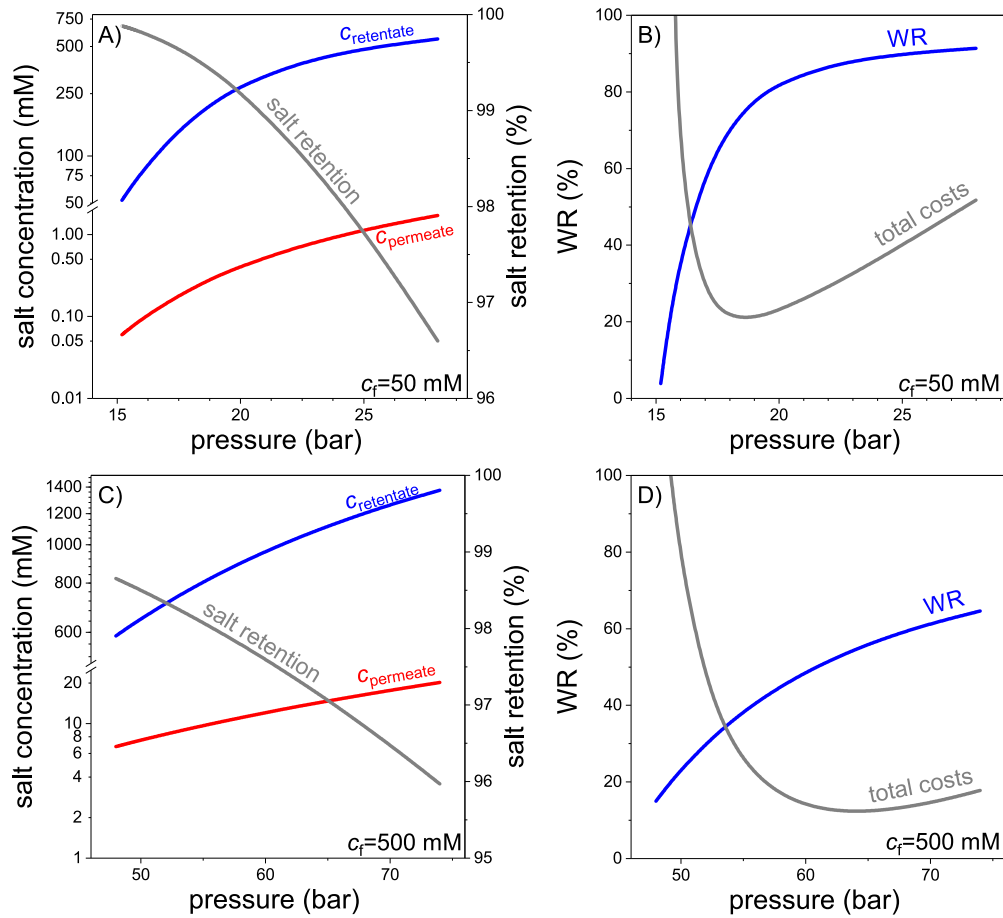
Fig. 13. Calculations for a 2D RO module for fixed water productivity of 20 LMH and 50 mM 1:1 salt solution as feed (A and B) or a 500 mM solution (C and D). Other parameters as in Fig. 12.
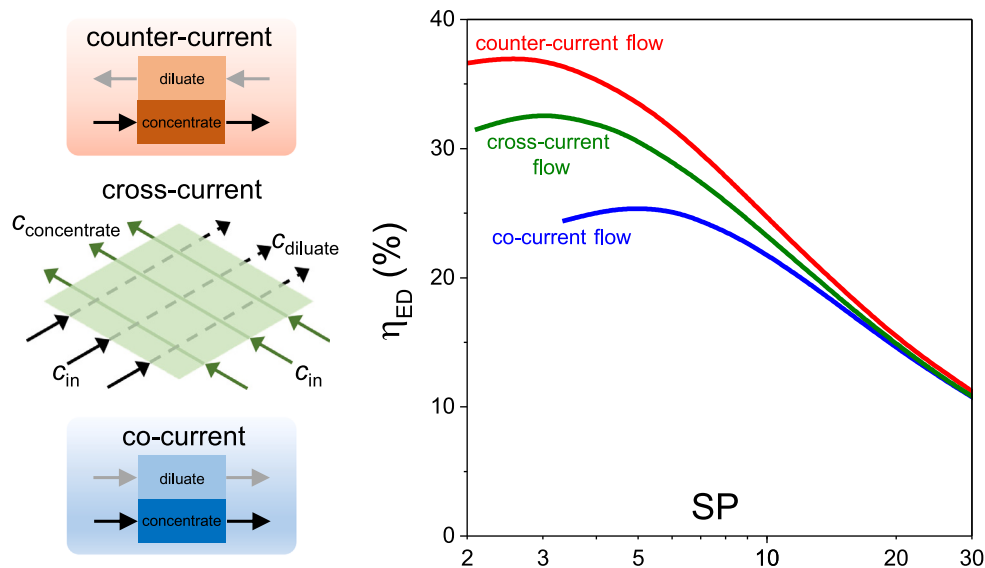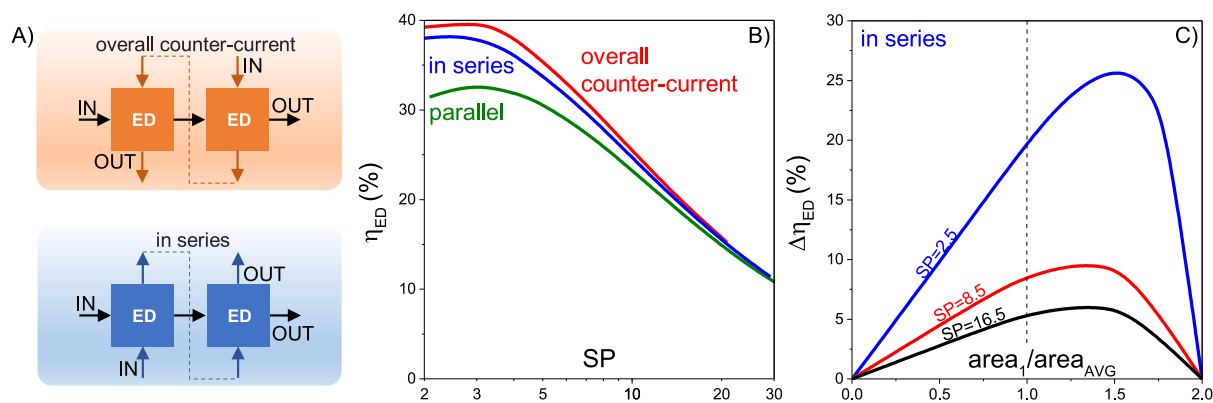

Fig. 14. Comparison of three flow patterns in an ED module, namely counter-current, cross-current, and co-current flow. Calculation results for an ED module based on input parameters from Section 4, evaluated as efficiency η_{ED} versus specific productivity, SP. All calculations for desalination from 500 to 50 mM, at a water recovery of 50%.

Fig. 15. Comparison of different methods of stacking two ED modules. Each individual stack is described by the 2D cross-current geometry. (A). Explanation of in-series and counter-current process layout. (B) Energy efficiency, η_{ED}, for three possible process layout schemes. (C). Relative increase in η_{ED} for the in-series layout when we vary the relative sizes of the two stacks.

area to have the same system-level SP in this comparison. Results of this calculation are presented in Fig. 15. All calculations in this section are based on the most realistic module layout (flow pattern) which is cross-current flow. Thus calculations here are based on a 2D model for each separate module, and then two modules are jointly considered, and for each value of SP, all free parameters are varied to arrive at an optimized efficiency η_{ED}, such that the curves in Fig. 15 are optimal for any chosen mode of stacking.

In Fig. 15 the line for single module is the same as if we had two smaller modules each with half the area, placed next to one another (in parallel). Thus the 'parallel' line in Fig. 15 is the same as the line for cross-current flow in Fig. 14. The second line is for the two modules placed in series, one behind the other. The cell pair voltages in both modules can be changed, and the aim is to arrive at the required setpoint (desalination from 500 mM to 50 mM) with the lowest total energy investment. Finally, the upper line is for two modules that on the system-level are operated in counter-current (each module by itself is operated in cross-current). Clearly, at moderate SP-values we can increase efficiency by either of these system-level stacking options. Around SP ∼ 3, an improvement by about ∼25% is possible when we go from a single module to two (smaller) modules. Note that in each module the cell pair voltage must be chosen exactly right to obtain this advantage, otherwise efficiency can even be worse than in a single module.

In a next set of calculations, presented in Fig. 15C, we only analyze the 'in-series' system-geometry and change the sizes (i.e., membrane area) of the two modules, but still with overall the same system-level SP (i.e., if one module is made larger, the other must be made smaller), while we again optimize the two voltages in each module. Reported is the *relative* increase in efficiency compared to the situation of a single module. The two extremes, at the very left and very right in Fig. 15C refer to the single module, and the condition in the exact middle is the in-series geometry with two equally-sized modules. We notice that we can gain a further increase in efficiency if the first unit is increased in size by up to 50% and the second one made smaller by that same amount. Note that this change in size can simply be realized by having more cell pairs in the first, larger, unit, and less in the second, smaller, unit (with all water still flowing through both stacks), which increases the residence time in the first unit and reduces it in the second. At the lowest SP (upper curve), we can have a relative efficiency increase (relative to the single module) of ∼25%. The improvement compared to the case of two equally-sized modules (at the vertical dashed line) is relatively modest, not more than about 5%, but nevertheless it might pay off to increase the number of cell pairs in the first unit, and reduce this number in the second unit.

6.5. 3D Cross-current ED model with concentration polarization

In this final section we further increase the level of detail of the model for an ED module, by including concentration polarization (CP). In a simplified model without CP, at each macroscopic position in the module we have across the height of the channel a constant salt concentration, i.e., in this direction we have perfect mixing ('crosschannel mixing'). In the full 3D cross-current model that includes CP, we solve the Nernst–Planck equation for each ion, not only in the membrane, but also across the height of the channel, resulting in a description of the development of concentration profiles in this direction, and thus different concentrations are calculated at the membrane surface relative to the center of the channel, i.e., we now include concentration polarization. In the numerical 3D calculation, space is discretized in all three directions into a large number of gridpoints. At any distance from the membrane, water flows along the membrane in the required direction from inlet to outlet, also advecting ions with it. At the same time, by diffusion and electromigration ions also move towards, or away from, the membranes. We assume plug flow for the water, i.e., at each position we have the same velocity of water in the direction along the membranes. We neglect water flow through the membrane, and in that regard the membranes are ideal. However, we do include that the membranes are leaky for coions, as discussed at length in Section 4, and this is an important modeling element. We assume steady-state and an ED cell with unsegmented electrodes, i.e., at each position in the stack there is only one cell pair voltage, which is the same as the approach in previous sections. Parameters are: membrane charge density $X = 4.0$ M, membrane ion transfer coefficient $k_m = 0.24$ μm/s, channel thickness $L_{ch} = 200$ μm, and ion diffusion coefficient in the flow channel $D_{ch} = 1 \cdot 10^{-9}$ m²/s, which includes a porosity and tortuosity effect.

For many conditions, we notice that significant concentration profiles develop across the height of the channel, sometimes up to a factor ∼4 difference in concentration between the center of a channel and the channel/membrane interface. Because of these concentration profiles the resistance across the diluate channel goes up somewhat but this is a small effect. Much more important are two other effects related to the membranes. First of all, CP increases the Donnan potential on the diluate/membrane interface (more than it reduces the Donnan potential on the other side), because the salt concentration at the channel/membrane interface is now much lower. For this reason the cell pair voltage goes up and thus the energy consumption. But another effect is even more important. Because of the decreasing concentration in the diluate channel at the channel/membrane interface, and likewise the increasing concentration on the concentrate side, salt leakage from the concentrate channels significantly increases, which lowers current
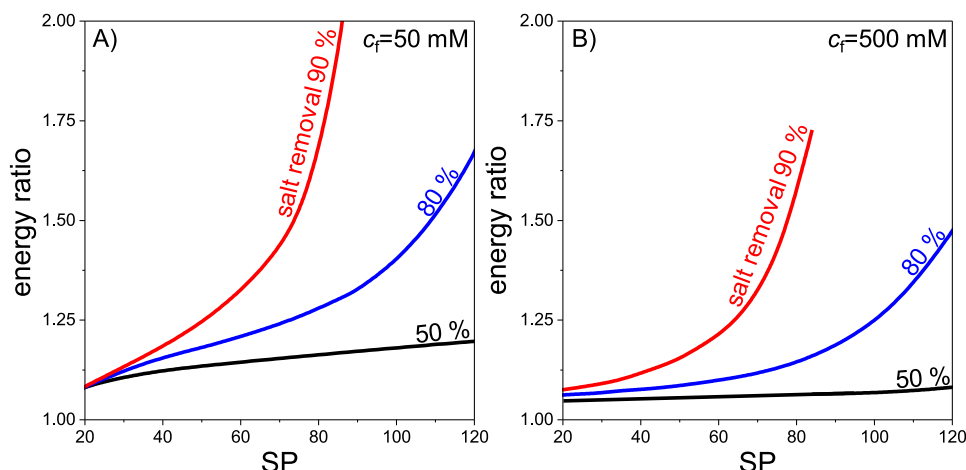
Fig. 16. Calculations for ED with 3D cross-current geometry and non-ideal membranes, with and without concentration polarization (CP). For two values of feed salt concentration and three values of salt removal (percentage-wise reduction in diluate salt concentration), results are presented for the energy ratio as function of specific productivity, SP. The energy ratio is the calculated energy use to reach the required salt removal when we do include CP (which is a more precise model) over a model that neglects CP (a model based on the assumption of 'crosschannel mixing').

efficiency, λ. Now, because we need to arrive at the same setpoint of a certain salt removal, to compensate for this leakage, currents must be increased, and this also leads to higher voltages. This increased leakage, and the required compensation for it such that we arrive at the same setpoint, is the key reason why if we include CP in a model in which membranes are leaky for co-ions, we have a significantly larger energy consumption, in some of the calculations reported in Fig. 16 up to a factor of two more.

Calculations are performed at many values of the specific productivity, SP, and in each calculation the cell pair voltage is adjusted until a certain salt removal is achieved. Based on the average current density and energy use, the energy ratio is calculated, which is the theoretical energy use when the CP-effect is included, divided by the energy use based on an ED model without CP. The energy ratio is then a kind of error that we make in a calculation without CP, where a more accurate analysis should have included CP. One can also conceive of the energy ratio as the technological potential to reduce energy consumption by developing ED channel designs that reduce the CP effect. Thus we present in Fig. 16 results of the energy ratio, for different values of salt removal and feed salt concentration as function of SP. These energy ratios are always beyond one, and this implies that an ED module including CP always needs more energy than without CP, to arrive at the same salt removal. As Fig. 16 shows, for low productivity, and moderate salt removal (50%), the energy ratio is not too far from unity. However, for a higher salt removal calculations show energy ratios going up to values of two. Thus, at high SP and high salt removal (above 80%), CP is important and significantly increases the energy use. Thus, both for low and high feed salt concentration, the effect of CP can be very significant when we simultaneously aim for a high salt removal and high productivity.

7. Conclusions and outlook

In this tutorial review, we have presented theory for reverse osmosis and electrodialysis, explaining how both technologies are based on fundamental transport theory, and illustrating their application in simple geometries, complete modules, and in system optimization of multiple combined units. For RO we discussed the solution-friction model which predicts a limiting retention at a high permeate water flux. For a 2D module, an analytical result was derived when advection dominates that leads to a simple model of RO for neutral solutes, that can be used in cost optimization studies. For ED we develop new equations

for Donnan equilibrium that extend the standard ideal expression. We present analytical equations for current efficiency, showing that this is a process parameter, not a membrane material property. We analyze combination of multiple modules in a system, and explain that for RO there can be a positive effect but only at a low permeate water flux. For ED, it can be useful to couple multiple modules, but only if membranes are relatively inexpensive and we can work at high energy efficiency. Concentration polarization in ED has a small effect when salt removal is below 80%, but must be included when a larger concentration reduction must be achieved.

As an outlook, let us summarize a few topics that we did not address. First of all, it is important to study how to extend both in RO and ED from simple 1:1 salt solutions to multi-ionic solutions. Even the addition of one extra type of anion or cation significantly changes the entire modeling framework. In addition, in real water sources also the protonation degree of ions must be considered, which depends on local pH. At high concentrations, ions also associate in ion pairs. These effects are relevant to study because for instance an ammonium ion is acted on by the electrical field, but the neutral ammonia species, is not. Thus retention of these ions is strongly pH-dependent. For very tiny pores, a related topic is the effective size of ions, that has an impact on their partitioning and their mobility within the membranes. Ions with a higher charge will be hydrated better, and are expected to be slower. State-of-the-art theory for simultaneous transport and reaction of ions (such as acid–base reactions between ions) assumes that these reactions are very fast, but it is interesting to study if that is a correct assumption. Another important assumption is local electroneutrality in channels and in membranes. Especially in reverse osmosis where membranes can be as thin as 100 nm, it is important to know if Poisson's equation must be used to replace the assumption of local electroneutrality in the membrane.

Other topics of relevance are the use of NF and RO to remove organic micropollutants (OMPs) and other charged molecules such as perfluoroalkyl substances (PFAS). A very different topic is the theoretical study of electro-deionization (EDI), which is an ED system with channels containing (mixed bed) resin particles to reduce energy costs and produce ultra-pure water. In the theory for EDI we may have to include water-splitting reactions at points where acidic and basic resin particles touch.

Nomenclature

Symbols		
a	Specific membrane surface area, $a = 1/L_{ch}$	m^{-1}
A	Membrane area	m^2
$c_{i,j}$	Concentration of solute or ion i in stream j[a]	mol/m^3
$c_{m,i}$	Concentration of ion i in membrane	mol/m^3
$c_{T,m}$	Total concentration of all ions together in the membrane	mol/m^3
CMP	Costs of material purchase	
CUE	Costs of a unit of energy	
$D_{m,i}$	Membrane-based diffusion coefficient, $D_{m,i} = \varepsilon D_{\infty,i}$	m^2/s
e_{min}	Theoretical minimum energy of a desalination process	W
ec_{min}	$ec_{min} = E_{min}/\Pi_f$	
E_{min}	Theoretical minimum energy of desalination per m^3 of freshwater produced	J/m^3
f	Dimensionless z-dependent upstream flowrate, $f = \phi_v(z)/\phi_{v,f}$	
F	Faraday's constant (96485 C/mol)	C/mol
$\mathcal{F}_{driving,i}$	Driving force on ion i	J/mol/m
$\mathcal{F}_{friction,i}$	Friction force on ion i	J/mol/m
$f_{elec,j}$	Contribution to the free energy density of a solution by Coulomb interactions between ions	J/m^3
$f_{F\text{-}m}$	Friction of water with the membrane matrix	$mol \cdot s/m^5$
$f^*_{i\text{-}j}$	Friction factor of ion i with another ion j	$J.s/mol/m^2$
$f^*_{i\text{-}m}$	Friction factor of an ion with the membrane matrix	$J.s/mol/m^2$
$f^*_{i\text{-}w}$	Friction factor of an ion with water	$J.s/mol/m^2$
I	Current or current density	A, or A/m^2
J_i	Transmembrane molar flow rate of solutes[b]	$mol/m^2/s$
k_B	Boltzmann's constant ($1.3806\ 10^{-23}$ J/K)	J/K
k_{ch}	Channel mass transfer coefficient, $k_{ch} = \varepsilon D_\infty/L_{ch}$	(m/s)
$k_{F\text{-}m}$	Water–membrane permeability, $k_{F\text{-}m} = \mathbb{k}_{F\text{-}m}/L_m = L_m/f_{F\text{-}m}$	$m^4/mol \cdot s$
$k_{m,i}$	Membrane mass transfer coefficient, $k_{m,i} = D_{m,i}/L_m$	m/s
$K_{f,i}$	Function describing solute–membrane friction	
L_{ch}	Flow channel thickness	m
L_m	Membrane thickness	m
m_1, m_2	Multiplier for total energy use; multiplier for other plant expenses	
N_{av}	Avogadro's number ($6.0221\ 10^{23}$ mol^{-1})	mol^{-1}
n_i	Ion concentration in numbers per volume	m^{-3}
p	Membrane porosity	
P^h	Hydrostatic pressure	Pa (bar)
P_i	Passage of ion or solute i, $P_i = 1 - R_i$	
Pe_i	Membrane Péclet-number, $Pe_i = v_F/k_{m,i}$	
R	Gas constant (8.3144 J/mol/K)	J/mol/K
R_i	Retention (or rejection) of ion or solute i	
S_i	Solubility (same as Φ_i)	
S_j	Entropy associated with a certain water flow	J/s/K
SP	Specific productivity, a measure of average transmembrane water flow rate	
T	Temperature	K
t^*	Time-on-stream, $t^* = z/v_z$	s
tc	Dimensionless total costs	
TC	Total costs per time in operation	
V_{cp}	Cell pair voltage	V
v_w	Transmembrane water velocity, permeate water flux[b]	m/s
V_T	Thermal voltage, $V_T = RT/F$	V
v_z	Velocity of water through a channel, i.e., along membrane	m/s
WR	Water recovery	
x	Coordinate towards and across membrane	
$\lvert X \rvert$	Magnitude of the membrane charge density	mol/m^3
z	Direction along membrane	
α_1, α_2	Over-pressurization factors	
Δc	Extent of desalination (difference in salt concentration between feedwater and product water, $\Delta c = c_f - c_p$)	mM
$\Delta P^{h,\infty}$	Hydrostatic pressure difference across the membrane	Pa (bar)
Δt	Membrane lifetime	s
$\Delta\phi_{ch,j}$	Potential drop across channel j (dimensionless)	
$\Delta\phi_{Donnan,j}$	Donnan potential at solution/membrane interface	
$\Delta\phi_{Donnan,tot}$	Total Donnan potential across a membrane	
$\Delta\phi_m$	Potential drop across the inner coordinates of the membrane	
ε	$\varepsilon = p/\tau$	
η	Energy efficiency, ratio of theoretical minimum energy to achieve a certain desalination over the actual energy investment (also called TEE, thermodynamic energy efficiency)	
λ_B	Bjerrum length	m
λ_{cp}	Current efficiency	
μ_i	Chemical potential of an ion	J/mol
$\mu_{aff,i}$	Contribution of affinity to the chemical potential of an ion with a certain phase	J/mol
$\mu_{exc,i}$	Contribution of volumetric interactions to the chemical potential of an ion	J/mol
$\mu_{ref,i}$	Reference value relevant when ions are part of chemical reactions	J/mol
v_i	Molar volume of an ion	m^3/mol
$v_i P^{tot}$	Pressure insertion term	J/mol
Π	Osmotic pressure of a solution	Pa (bar)

$\Pi_{\text{dbl/mem}}$	Osmotic pressure at the interface between DBL and membrane	Pa (bar)
σ_i	Reflection coefficient, $\sigma_i = 1 - K_{\text{f},i}\Phi_i$	
τ	Tortuosity	
$\boldsymbol{\tau}$	Tortuosity factor of a porous structure $\boldsymbol{\tau} = \tau^2$	
ϕ	Volume fraction of all ions together	
ϕ_{v}	Volumetric flowrate	m^3/s
Φ_i	Partitioning coefficient (same as S_i)	
ξ	Dimensionless coordinate along the membrane from inlet to outlet (0 to 1)	
ω	Sign of the membrane charge density	
Subscripts		
c	concentrate (in RO: retentate)	
f	feedwater	
p	product water, or freshwater (in RO: permeate)	
∞	conditions outside of membrane, or salt concentration in solution for a $z{:}z$ salt	

aThe words 'ion' and 'solute' are interchangeably used in this table.

bThese fluxes across the membrane are defined per unit geometrical 'outer' area of a membrane, i.e., they are defined as superficial velocities, not interstitial. This means they are not defined for instance per cross-sectional area of the pores only.

Declaration of competing interest

The authors declare that they have no known competing financial interests or personal relationships that could have appeared to influence the work reported in this paper.

References

[1] M. Elimelech, W.A. Philip, The future of seawater desalination: Energy, technology, and the environment, Science 333 (2011) 712–717.

[2] A. Campoine, L. Gurreri, M. Ciofalo, G. Micale, A. Tamburini, A. Cipollina, Electrodialysis for water desalination: A critical assessment of recent developments on process fundamentals, models and applications, Desalination 434 (2018) 121–160.

[3] A. Yaroshchuk, M.L. Bruening, E. Zholkovskiy, Modelling nanofiltration of electrolyte solutions, Adv. Colloid Interface Sci. 268 (2019) 39–63.

[4] V. Freger, G.Z. Ramon, Polyamide desalination membranes: Formation, structure, and properties, Prog. Polym. Sci. 122 (2021) 101451.

[5] V.M. Starov, N.V. Churaev, Separation of electrolyte solutions by reverse osmosis, Adv. Colloid Interface Sci. 43 (1993) 145–167.

[6] K. Arola, A. Ward, M. Mänttäri, M. Kallioinen, D. Batstone, Transport of pharmaceuticals during electrodialysis treatment of wastewater, Water Res. 161 (2019) 496–504.

[7] A. Verliefde, E. Cornelissen, G. Amy, B. van der Bruggen, H. van Dijk, Priority organic micropollutants in water sources in Flanders and the Netherlands and assessment of removal possibilities with nanofiltration, Environ. Pollut. 146 (2007) 281–289.

[8] S. Lee, C. Boo, M. Elimelech, S. Hong, Comparison of fouling behavior in forward osmosis (FO) and reverse osmosis (RO), J. Membr. Sci. 365 (2010) 34–39.

[9] R. Ghalloussi, W. Garcia-Vasquez, L. Chaabane, L. Dammak, C. Larchet, S.V. Deabate, E. Nevakshenova, V. Nikonenko, D. Grande, Ageing of ion-exchange membranes in electrodialysis: A structural and physicochemical investigation, J. Membr. Sci. 436 (2013) 68–78.

[10] L. Gurreri, A. Filingeri, M. Ciofalo, A. Cipollina, M. Tedesco, A. Tamburini, G. Micale, Electrodialysis with asymmetrically profiled membranes: Influence of profiles geometry on desalination performance and limiting current phenomena, Desalination 506 (2021) 115001.

[11] J.R. Werber, A. Deshmukh, M. Elimelech, Can batch or semi-batch processes save energy in reverse-osmosis desalination? Desalination 402 (2017) 109–122.

[12] P.M. Biesheuvel, The activity coefficient of $z{:}1$ ionic solutions scales with the cube root of salt concentration, 2020, arXiv:2012.12194.

[13] P.M. Biesheuvel, M. van Soestbergen, Counterion volume effects in mixed electrical double layers, J. Colloid Interface Sci. 316 (2007) 490–499.

[14] E.M. Kimani, A.J.B. Kemperman, W.G.J. van der Meer, P.M. Biesheuvel, Multicomponent mass transport modeling of water desalination by reverse osmosis including ion pair formation, J. Chem. Phys. 154 (2021) 124501.

[15] L. Wang, C. Violet, R.M. DuChanois, M. Elimelech, Derivation of the theoretical minimum energy of separation of desalination processes, J. Chem. Educ. 97 (2020) 4361–4369.

[16] O. Kedem, V. Freger, Determination of concentration-dependent transport coefficients in nanofiltration: Defining an optimal set of coefficients, J. Membr. Sci. 310 (2008) 586–593.

[17] J.G. Gamaethiralalage, K. Singh, S. Sahin, J. Yoon, M. Elimelech, M.E. Suss, P. Liang, P.M. Biesheuvel, R.L. Zornitta, L.C.P.M. de Smet, Recent advances in ion selectivity with capacitive deionization, Energy Env. Sci. 14 (2021) 1095–1120.

[18] W.R. Bowen, J.S. Welfoot, Modelling the performance of membrane nanofiltration – Critical assessment and model development, Chem. Eng. Sci. 57 (2002) 1121–1137.

[19] K.S. Spiegler, O. Kedem, Thermodynamics of hyperfiltration (reverse osmosis): Criteria for efficient membranes, Desalination 1 (1966) 311–326.

[20] H.K. Lonsdale, U. Merten, R.L. Riley, Transport properties of cellulose acetate osmotic membranes, J. Appl. Polym. Sci. 9 (1965) 1341–1362.

[21] D.R. Paul, Reformulation of the solution-diffusion theory of reverse osmosis, J. Membr. Sci. 241 (2004) 371–386.

[22] J.G. Wijmans, R.W. Baker, The solution-diffusion model: A review, J. Membr. Sci. 107 (1995) 1–21.

[23] E.H. Bresler, L.J. Groome, On equations for combined convective and diffusive transport of neutral solute across porous membranes, Am. J. Physiol. 241 (1981) F469–F476.

[24] A. Yaroshchuk, "Breakthrough" osmosis and unusually high power densities in pressure-retarded osmosis in non-ideally semi-permeable supported membranes, Sci. Rep. 7 (2017) 45168.

[25] O. Kedem, A. Katchalsky, A physical interpretation of the phenomenological coefficients of membrane permeability, J. Gen. Physiol. 45 (1961) 143–179.

[26] G.S. Manning, Binary diffusion and bulk flow through a potential-energy profile: A kinetic basis for the thermodynamic equations of flow through membranes, J. Chem. Phys. 49 (1968) 2668–2675.

[27] X.L. Wang, T. Tsuru, S.I. Nakao, S. Kimura, The electrostatic and steric-hindrance model for the transport of charged solutes through nanofiltration membranes, J. Membr. Sci. 135 (1997) 19–32.

[28] H. Chmiel, X. Lefebvre, V. Mavrov, M. Noronha, J. Palmeri, Computer simulation of nanofiltration, membranes and processes, in: M. Rieth, W. Schommers (Eds.), in: Handbook of Theoretical and Computational Nanotechnology, vol. 5, American Scientific Publishers, 2006, pp. 93–214.

[29] I. Sutzkover, D. Hasson, R. Semiat, Simple technique for measuring the concentration polarization level in a reverse osmosis system, Desalination 131 (2000) 117–127.

[30] S. Bhattacharjee, J.C. Chen, M. Elimelech, Coupled model of concentration polarization and pore transport in crossflow nanofiltration, AIChE J. 47 (2001) 2733–2745.

[31] J.R. Pappenheimer, Passage of molecules through capillary walls, Physiol. Rev. 33 (1953) 387–423.

[32] A.A. Sonin, Osmosis and ion transport in charged porous membranes: A macroscopic, mechanistic model, in: E. Sélégny (Ed.), Charged Gels and Membranes I, D. Reidel, Dordrecht, 1976, pp. 255–265.

[33] L. Wang, T. Cao, J.E. Dykstra, S. Porada, P.M. Biesheuvel, M. Elimelech, Salt and water transport in reverse osmosis membranes: Beyond the solution-diffusion model, Environ. Sci. Technol. 55 (2021) 16665–16675.

[34] J.L. Anderson, D.M. Malone, Mechanism of osmotic flow in porous membranes, Biophys. J. 14 (1974) 957–982.

[35] J.G. Wijmans, S. Nakao, J.W.A. van den Berg, F.R. Troelstra, C.A. Smolders, Hydrodynamic resistance of concentration polarization boundary layers in ultrafiltration, J. Membr. Sci. 22 (1985) 117–135.

[36] P. Bacchin, Colloid-interface interactions initiate osmotic flow dynamics, Coll. Surf. A 533 (2017) 147–158.

[37] V. Sasidhar, E. Ruckenstein, Electrolyte osmosis through capillaries, J. Colloid Interface Sci. 82 (1981) 439–457.

[38] A. Katchalsky, P.F. Curran, Nonequilibrium Thermodynamics in Biophysics, Harvard University Press, Cambridge, MA, USA, 1965.

[39] P.M. Biesheuvel, J.E. Dykstra, Physics of Electrochemical Processes, ISBN: 9789090332581, 2020.

[40] A. Zhu, P.D. Christofides, Y. Cohen, Effect of thermodynamic restriction on energy cost optimization of RO membrane water desalination, Ind. Eng. Chem. Res. 48 (2009) 6010–6021.

[41] Q.J. Wei, R.K. McGovern, J.H. Lienhard, Saving energy with an optimized two-stage reverse osmosis system, Environ. Sci. Water Res. Technol. 3 (2017) 659–670.

[42] M. Tedesco, H.V.M. Hamelers, P.M. Biesheuvel, Nernst–Planck transport theory for (reverse) electrodialysis: III. Optimal membrane thickness for enhanced process performance, J. Membr. Sci. 565 (2018) 480–487.

[43] Y.L. Hwang, F.G. Helfferich, Generalized model for multispecies ion-exchange kinetics including fast reversible reactions, React. Polym. 5 (1987) 237–253.

[44] K.M. Chehayeb, K.G. Nayar, J.H. Lienhard, On the merits of using multi-stage and counterflow electrodialysis for reduced energy consumption, Desalination 439 (2018) 1–16.

[45] J.C. Fair, J.F. Osterle, Reverse electrodialysis in charged capillary membranes, J. Chem. Phys. 54 (1971) 3307–3316.

[46] A.G. Guzmán-Garcia, P.N. Pintauro, M.W. Verbrugge, R.F. Hill, Development of a space-charge transport model for ion-exchange membranes, AIChE J. 36 (1990) 1061–1074.

[47] S. Basu, M.M. Sharma, An improved space-charge model for flow through charged microporous membranes, J. Membr. Sci. 124 (1997) 77–91.

[48] Y. Yang, P.N. Pintauro, Multicomponent space-charge transport model for ion-exchange membranes with variable pore properties, Ind. Eng. Chem. Res. 43 (2004) 2957–2965.

[49] P.B. Peters, R. van Roij, M.Z. Bazant, P.M. Biesheuvel, Analysis of electrolyte transport through charged nanopores, Phys. Rev. E 93 (2016) 053108.

[50] R. Schlögl, Zur Theorie der anomalen Osmose, Z. Phys. Chem. 3 (1955) 73–102.

[51] M.W. Verbrugge, R.F. Hill, Ion and solvent transport in ion-exchange membranes. I. A macrohomogeneous mathematical model, J. Electrochem. Soc. 137 (1990) 886–893.

[52] J.A.M. Kuipers, K.J. van Duin, F.P.H. van Beckum, W.P.M. van Swaaij, A numerical model of gas-fluidized beds, Chem. Eng. Sci. 47 (1992) 1913–1924.

[53] P.M. Biesheuvel, Two-fluid model for the simultaneous flow of colloids and fluids in porous media, J. Colloid Interface Sci. 355 (2011) 389–395.

[54] M. Tedesco, H.V.M. Hamelers, P.M. Biesheuvel, Nernst–Planck transport theory for (reverse) electrodialysis: II. Effect of water transport through ion-exchange membranes, J. Membr. Sci. 531 (2017) 172–182.

[55] Y.S. Oren, P.M. Biesheuvel, Theory of ion and water transport in reverse osmosis membranes, Phys Rev. Appl. 9 (2018) 024034.

[56] T. Teorell, Transport phenomena in membranes. Eighth spiers memorial lecture, Discuss. Faraday Soc. 21 (1956) 9–26.

[57] A. Mauro, Nature of solvent transfer in osmosis, Science 126 (1957) 252–253.

[58] P.M. Ray, On the theory of osmotic water movement, Plant Physiol. 35 (1960) 783–795.

[59] A. Mauro, Osmotic flow in a rigid porous membrane, Science 149 (1965) 867–869.

[60] A.H. Galama, J.W. Post, M.A. Cohen Stuart, P.M. Biesheuvel, Validity of the Boltzmann equation to describe Donnan equilibrium at the membrane-solution interface, J. Membr. Sci. 442 (2013) 131–139.

[61] D. Brogioli, A. Vailati, Diffusive mass transfer by nonequilibrium fluctuations: Fick's law revisited, Phys. Rev. E 63 (2000) 012105.

[62] L. Song, Thermodynamic modeling of solute transport through reverse osmosis membrane, Chem. Eng. Comm. 180 (2000) 145–167.

[63] P.M. Biesheuvel, J.E. Dykstra, S. Porada, M. Elimelech, New parametrization method for salt permeability of reverse osmosis desalination membranes, J. Membr. Sci. Lett. 100010 (2022).

[64] K. Kezia, J. Lee, A.J. Hill, S.E. Kentish, Convective transport of boron through a brackish water reverse osmosis membrane, J. Membr. Sci. 445 (2013) 160–169.

[65] P.M. Biesheuvel, L. Zhang, P. Gasquet, B. Blankert, M. Elimelech, W.G.J. van der Meer, Ion selectivity in brackish water desalination by reverse osmosis: Theory, measurements, and implications, environ, Sci. Technol. Lett. 7 (2020) 42–47.

[66] M.S. Hall, V.M. Starov, D.R. Lloyd, Reverse osmosis of multicomponent electrolyte solutions Part I. Theoretical development, J. Membr. Sci. 128 (1997) 23–37.

[67] T. Tsuru, S. Nakao, S. Kimura, Calculation of ion rejection by extended Nernst–Planck equation with charged reverse osmosis membranes for single and mixed electrolyte solution, J. Chem. Eng. Japan 24 (1991) 511–517.